

Chapter 5

Development of high-throughput assays for characterising a library of *P. falciparum* merozoite surface proteins

5.1 INTRODUCTION

5.1.1 Cell surface proteins of the human erythrocyte.

The cell surface protein repertoire of human erythrocytes has been studied extensively over the past five decades and more than 300 membrane-associated proteins have now been identified with the use of high-resolution mass-spectrometry based approaches (Kakhniashvili *et al.*, 2004; Pasini *et al.*, 2006; Speicher, 2006; Pasini *et al.*, 2010). Proteomic studies of erythrocyte membranes have revealed a very broad range of protein expression levels, with the highly abundant proteins such as Glycophorin A and Band 3 being present at $\sim 10^6$ copies/cell and others with very low abundance, including CR1, being available only at a few hundred copies/cell (Pasini *et al.*, 2006). Lateral diffusion of membrane proteins along the plane of the lipid bilayer has been demonstrated to be restricted in certain cases by direct or indirect interactions with the spectrin-based cytoskeleton, which likely facilitates compartmentalisation of these proteins in specialised membrane domains such as the cholesterol-rich lipid rafts (Koppel *et al.*, 1981; Tomishige *et al.*, 1998). Proteins resident in lipid rafts have been observed to be recruited to the host-derived parasitophorous vacuolar membrane that surrounds the intra-erythrocytic stages of *Plasmodium* and are proposed to be important for parasite entry (Murphy *et al.*, 2006).

5.1.2 The role of host-cell surface multi-pass membrane proteins in the invasion of erythrocytes by *Plasmodium* merozoites.

Multi-pass membrane proteins, comprising of two or more transmembrane domains, account for a major fraction of the total surface protein complement of the human erythrocyte. Many of these act as transporters and play important roles in nutrient import, regulation of cell volume and ionic balance (Pasini *et al.*, 2006). A few of the multi-pass proteins, including the Duffy antigen

receptor for chemokines, Aquaporin 1 and Glucose transporter 1 are enriched in lipid rafts and trafficked to the parasitophorous vacuole of *Plasmodium* (Murphy *et al.*, 2006).

A definitive role in erythrocyte invasion by *Plasmodium* has so far been identified only for one multi-pass protein, the Duffy antigen, a seven transmembrane G protein-coupled protein that also acts as a promiscuous receptor for several chemokines (Barnwell *et al.*, 1989; de Brevern *et al.*, 2005). The interaction of the Duffy antigen with the Duffy binding protein (DBP) from *P. vivax* and *P. knowlesi* is critical for invasion of human erythrocytes by these parasites. The Region II (RII) of the DBP ectodomain containing a single DBL (Duffy binding-like) domain is sufficient for binding to Duffy (Chitnis and Miller, 1994). Most of the biochemical characterisation of the Duffy-DBP interaction has been performed using recombinantly expressed DBP RII. Antibodies directed against PvDBP RII inhibit erythrocyte invasion by the parasite *in vitro* and provide clinical protection against *P. vivax* infection in children, therefore PvDBP RII is currently a leading vaccine candidate against *P. vivax* malaria (Grimberg *et al.*, 2007; King *et al.*, 2008). A single point mutation in the upstream promoter region of the Duffy gene (T→C, at position -33) that confers resistance from *P. vivax* and *P. knowlesi* infection by abolishing expression of the receptor, has been observed to be under strong positive selection in a number of human populations, reaching almost fixation in west and central Africa (Miller *et al.*, 1975; Miller *et al.*, 1976; Zimmerman *et al.*, 1999). A 35-amino acid peptide comprising residues 8-42 of the N-terminal extracellular region of Duffy has been shown to inhibit the binding of *P. vivax* DBP (PvDBP) to human erythrocytes, indicating the involvement of the corresponding region of the Duffy antigen in PvDBP recognition (Chitnis *et al.*, 1996). This region of Duffy also carries the antigenic determinant of the Fy^a and Fy^b blood groups. The Fy^a and Fy^b forms are characterised by Asp and Gly at position 42 respectively and a recent study has demonstrated ~50% lower

binding of PvDBP to Fy^a in comparison to Fy^b (King *et al.*, 2011). The Duffy antigen was previously thought to be essential for the invasion of human erythrocytes by *P. vivax*, but the recent identification of *P. vivax* infections in Duffy-negative individuals in Madagascar has called this universality into question (Ménard *et al.*, 2010).

The Duffy antigen, while perhaps not essential, clearly plays a crucial function in *P. vivax* and *P. knowlesi* infections, however, a role for this multi-pass receptor has not yet been identified in erythrocyte invasion by *P. falciparum*.

Several independent lines of investigation have revealed a possible involvement of another multi-pass protein, Band 3, in *P. falciparum* infection. Band 3 consists of an N-terminal cytoplasmic domain linked to the spectrin-based cytoskeleton and a C-terminal transmembrane domain that functions as an anion transporter (Wang *et al.*, 1993; Beckmann *et al.*, 1998; Hassoun *et al.*, 1998). The precise number of membrane-spanning helices in the C-terminal domain of Band 3 is not known, but predictions from topology modelling range from 11-14 (Tanner, 1997; Ota *et al.*, 1998, Table 7). Invasion of human erythrocytes by *P. falciparum* has been observed to be inhibited by liposomes containing Band 3 and by a monoclonal antibody raised against Band 3 (Miller *et al.*, 1983; Okoye and Bennett, 1985; Clough *et al.*, 1995). Short peptides containing amino-acid stretches found in the extracellular regions of Band 3 have also been demonstrated to inhibit invasion of erythrocytes by *P. falciparum*, albeit at relatively high concentrations (Goel *et al.*, 2003). These Band 3 peptides have been seen to bind to processed fragments of MSP1, MSP1₄₂ and MSP1₁₉ but interestingly not to full-length MSP1, suggesting that processing of MSP1 is perhaps necessary for the interaction with Band 3 (Goel *et al.*, 2003). Apart from the studies of Band 3 mentioned above, the role of multi-pass receptors in the invasion of erythrocytes by *P. falciparum* has not been investigated.

5.1.3 The recognition of glycan moieties on erythrocyte surface receptors by *Plasmodium* ligands.

Many of the proteins on the erythrocyte surface membrane are glycosylated and structural polymorphisms in glycans form the basis of several blood groups such as ABH, Lewis, T and Tn (King, 1994). Sialic acid moieties displayed on erythrocyte receptors are known to play an important role in the invasion of human erythrocytes by *P. falciparum* and indeed, the recognition of erythrocyte receptors by *P. falciparum* proteins has classically been categorised as being either sialic acid-dependent or independent. Of the known erythrocyte receptor-parasite protein interactions, the recognition of Glycophorins A, B and C by their respective *P. falciparum* ligands are all dependent on the presence of terminal sialic acid moieties (Camus & Hadley, 1985; Maier *et al.*, 2002; Mayer *et al.*, 2009). The interactions of *P. falciparum* surface proteins with glycans other than sialic acid are, however, relatively unknown.

5.1.4 Strategies for detecting and characterising interactions between erythrocyte and *Plasmodium* merozoite surface proteins.

The traditional biochemical assays used for investigating the interactions between erythrocyte receptors and *Plasmodium* ligands are relatively time consuming and laborious and are not suitable for use in high-throughput screening.

The original approach used by Camus and Hadley (1985) to identify EBA175, involved incubation of radio-labelled spent *P. falciparum* culture supernatant with erythrocytes, elution of specifically-bound supernatant proteins in a high salt solution and analysis of eluted proteins by SDS-PAGE and autoradiography. In these first reported studies, non-adherent proteins were removed by washing alone. The specificity of the assay was later improved by centrifugation of erythrocytes through silicone oil, after incubation with parasite supernatant, to remove non-

bound and weakly-bound supernatant proteins (Tran *et al.*, 2005; Tham *et al.*, 2009). The sensitivity of the detection step has also been enhanced by incorporation of Western blot procedures with protein-specific immuno-probes (Mayer *et al.*, 2001; Narum *et al.*, 2002).

Erythrocyte rosetting assays have also been used to map the specific binding sites of erythrocyte receptors on their known *Plasmodium* ligands. For example the sufficiency of the DBL domain-containing RII of *PfEBA175* and *PvDBP* for erythrocyte binding was discovered by expressing fragments of the ectodomains of these proteins on the surface of COS cells and visually counting the aggregates (or rosettes) of erythrocytes around the transfected cells (Sim, 1995; Chitinis and Miller, 1994).

A simpler and less subjective approach for detecting binding of recombinant *Plasmodium* proteins to erythrocytes has recently been demonstrated using *PvDBP* RII as an example (Tran *et al.*, 2005). In this assay, a fluorescently-labelled anti-His antibody was used to detect the association of His tagged-*PvDBP* RII with erythrocytes by flow cytometry. This assay is amenable for use in high-throughput screening, however, the requirement for purified *Plasmodium* proteins at relatively high (~50 µg/ml) concentrations to achieve clear binding, (probably due to the Duffy antigen-DBP interaction being of low affinity, a common property of cell surface protein-protein interactions), is a major drawback.

5.1.5 Work described in this chapter.

The work in this chapter was aimed at applying new approaches to investigate the roles of multi-pass transmembrane proteins and glycans in *P. falciparum* erythrocyte recognition, both of which are under-explored as potential receptors. The library of *P. falciparum* merozoite surface proteins introduced in Chapter 1 (Section 1.13) has previously been screened against a panel of single-pass erythrocyte surface proteins, expressed as full-length ectodomain fragments, by

AVEXIS (Cecile Wright-Crosnier, unpublished data). The AVEXIS platform however requires all proteins to be expressed in soluble form and is therefore not applicable to erythrocyte multi-pass membrane proteins, which are difficult to express as correctly folded amphiphilic fragments. In this study, 33 of the highest-expressing merozoite surface proteins from the library were screened against 41 erythrocyte multi-pass receptors (including two isoforms each of three proteins), using a flow cytometry-based approach derived from the assay developed previously for detecting the association of EBA175 and RH5 proteins to human erythrocytes (Chapters 3 and 4). The multi-pass proteins were each individually expressed on the surface of HEK293E cells by transient transfection and then used as ‘baits’ for *P. falciparum* proteins that had been multimerised by immobilisation on fluorescent beads. Putative interactions between the merozoite proteins and the multi-pass receptors were detected using flow cytometry (Figure 43). Prior to probing against the multi-pass receptors, the merozoite proteins were pre-screened against erythrocytes for specific interactions. A small subset of selected merozoite proteins were also subsequently tested against a panel of synthetic carbohydrate probes in a preliminary screen to identify potential glycan-binding activities.

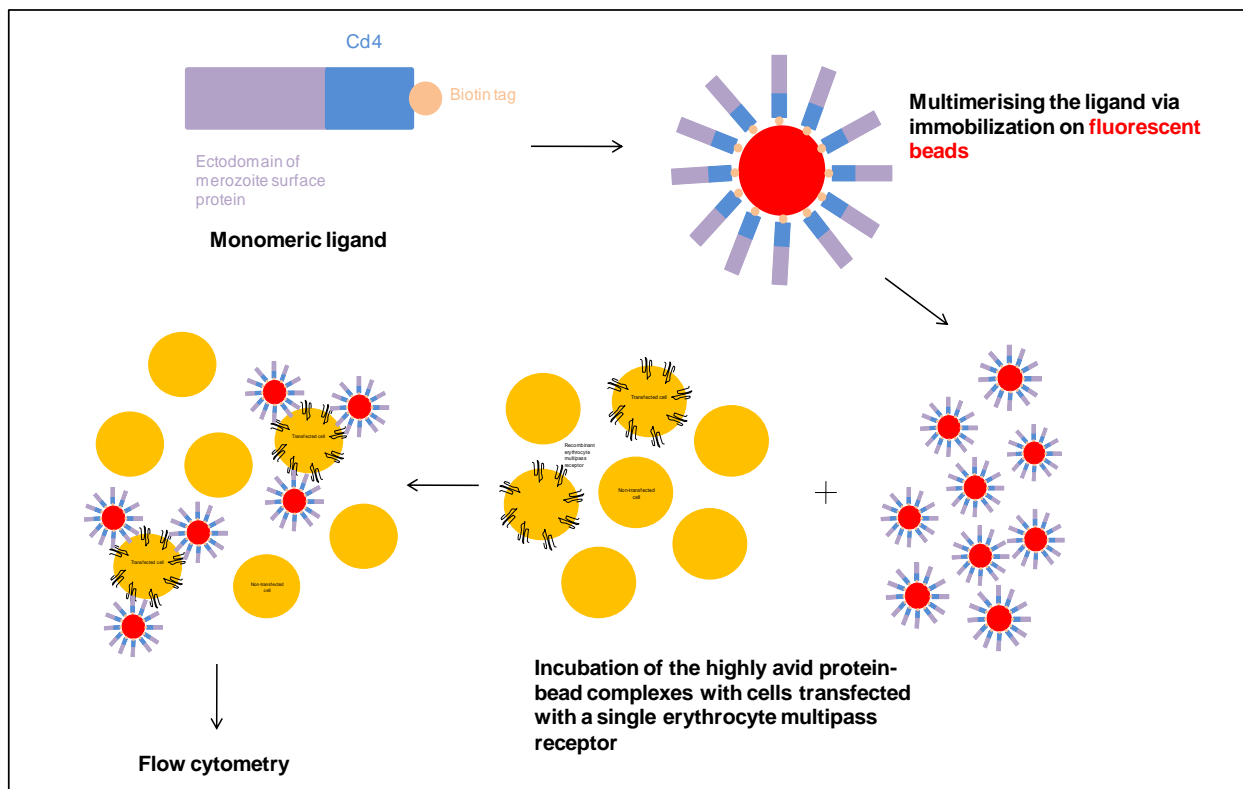


Figure 43. A schematic of the high-throughput screen used for identifying putative interactions between erythrocyte multi-pass receptors and *P. falciparum* merozoite surface proteins. In the screen, 33 merozoite surface proteins were tested individually against each of 41 erythrocyte multi-pass receptors. The ectodomain of each merozoite surface protein, produced recombinantly in fusion with rat Cd4 and a C-terminal biotin tag, was multimerised by clustering around streptavidin-coated Nile Red fluorescent beads. These multivalent ligand arrays were then be presented to HEK293E cells that had been transiently transfected with the expression construct for a single erythrocyte multi-pass receptor (in general only a certain fraction of the cell population displayed the recombinant multi-pass receptor , as transfection efficiency was < 100%) ; binding events were detected by flow cytometry.

5.2 RESULTS

5.2.1 40% of the *P. falciparum* merozoite surface proteins tested showed some association with human erythrocytes.

33 of the highest-expressing members of the *P. falciparum* merozoite surface protein library were selected for further characterisation in this study. Prior to testing against erythrocytes and recombinantly expressed erythrocytic multi-pass receptors, the merozoite proteins, produced in the monomeric form with C-terminal Cd4 and biotin tags, were immobilised on streptavidin-coated Nile red beads as described before (Chapter 3, Section 3.2.2). Multimerisation of the *Plasmodium* proteins on the bead-scaffolds was performed to potentially increase the avidity of their interactions with erythrocytic receptors, thereby prolonging them (increasing the half-lives) and facilitating their detection. The *Plasmodium* proteins were expressed using the HEK293E system and the cell culture supernatants containing the proteins were used in the assays with no pre-purification. The minimum amount of each protein necessary for saturating a uniform number of beads was assessed by ELISA individually (Figure 44). This assessment was deemed necessary, as non-saturation of beads with protein could decrease the avidity of the resulting arrays, whereas the presence of excess amounts of free (non-bead bound) protein could potentially act in an inhibitory manner against the binding of the arrays to erythrocytes.

The proteins arrayed on Nile red beads were presented to erythrocytes and binding was analysed by flow cytometry. The number of erythrocytes (as a percentage of total) binding to each protein was calculated based on a fluorescence intensity threshold, set with reference to the binding to Cd4-coated beads (negative control) and to EBA175-coated beads (positive control) (Figure 45 A). Although 13 out of the 33 proteins tested showed some association with erythrocytes, the

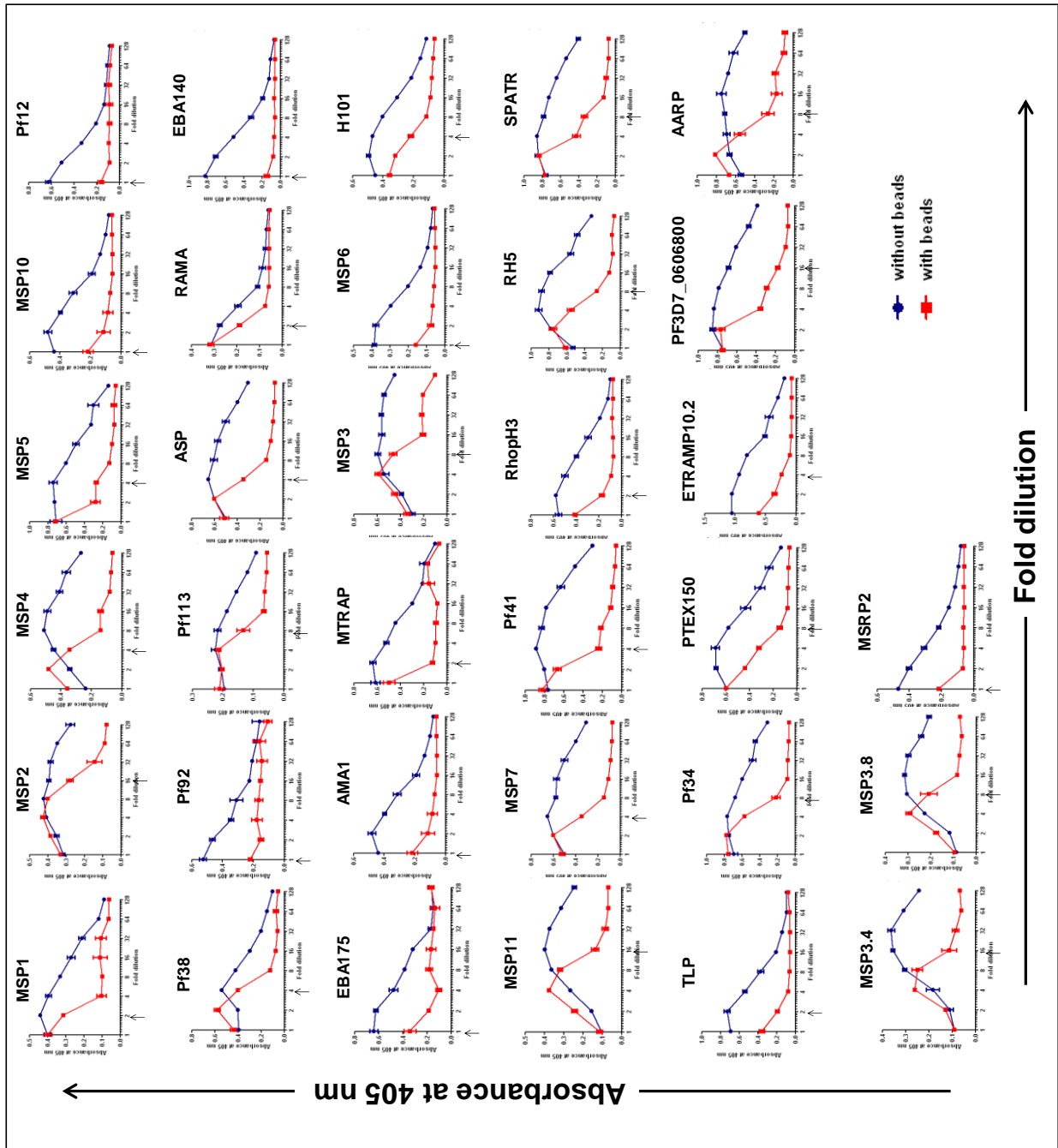


Figure 44. *P. falciparum* surface proteins were immobilised on streptavidin-coated beads to generate multivalent binding reagents for testing against surface receptors on erythrocytes and transiently-transfected HEK293E cells. 33 *P. falciparum* surface proteins, expressed with C-terminal Cd4 and biotin tags, were multimerised by direct attachment to streptavidin-coated Nile red beads. Cell culture supernatants containing the proteins were used for this purpose, with no prior purification step. The minimum amount of each protein necessary for complete saturation of a set number of beads was determined by performing ELISAs on 2-fold serially-diluted samples of the proteins, with and without pre-incubation with beads. The ELISAs were carried out on a streptavidin-coated plate, using OX68 as the primary antibody and an alkaline phosphatase-conjugated anti-mouse antibody as the secondary. Alkaline phosphatase activity was quantified by the turnover of the colorimetric substrate, *p*-nitrophenyl phosphate, measured as an increase in absorbance at 405 nm. Data is shown as mean \pm standard deviation; $n=3$. In the case of the protein samples pre-incubated with beads, a signal was expected to be seen in the ELISA, only when there was biotinylated protein in excess of what was needed for saturating the beads. The dilutions of the proteins selected for coating the beads, prior to presenting them to cells, is indicated by \uparrow .

variation in the binding responses was quite large, ranging from binding to ~80% of the cells down to ~2% of the cells (Figure 45). This is likely to reflect the availability/copy number of the erythrocytic receptors of the different *Plasmodium* proteins, as the highest binding was observed with the two *Plasmodium* proteins, EBA175 and EBA140 known to bind to two of the most abundant erythrocytic receptors Glycophorin A and Glycophorin C (~ 10^6 and 10^5 copies/cell respectively), whereas only 4% of the cells were observed to interact with RH5-coated beads, whose putative receptor BSG is expressed at a much lower level (Chapter 4, section 4.2.6).

The specificity of the binding of EBA175-coated beads to erythrocytes was previously tested by enzymatic pre-treatment of the cells with trypsin, chymotrypsin and neuraminidase (Chapter 3, section 3.2.2). The interaction of EBA140 with Glycophorin C is also known to be sensitive to trypsin and neuraminidase treatment but not to chymotrypsin treatment, whereas, the binding of RH5 to BSG is not affected by treatment with any of the three enzymes. To test whether the binding of EBA140 and RH5-coated beads to erythrocytes in this assay was specific, the cells were pre-treated with trypsin, chymotrypsin and neuraminidase, prior to incubation with the bead arrays. The results were consistent with the expected properties of these interactions (Figure 46). The specificity of the putative binding of the *P. falciparum* proteins Pf34, MSP3.4 and MSP3.8 was also tested by pre-treatment of erythrocytes with trypsin, chymotrypsin and neuraminidase. No significant reduction in the binding of these proteins to erythrocytes in response to any of the enzyme treatments was observed (data not shown).

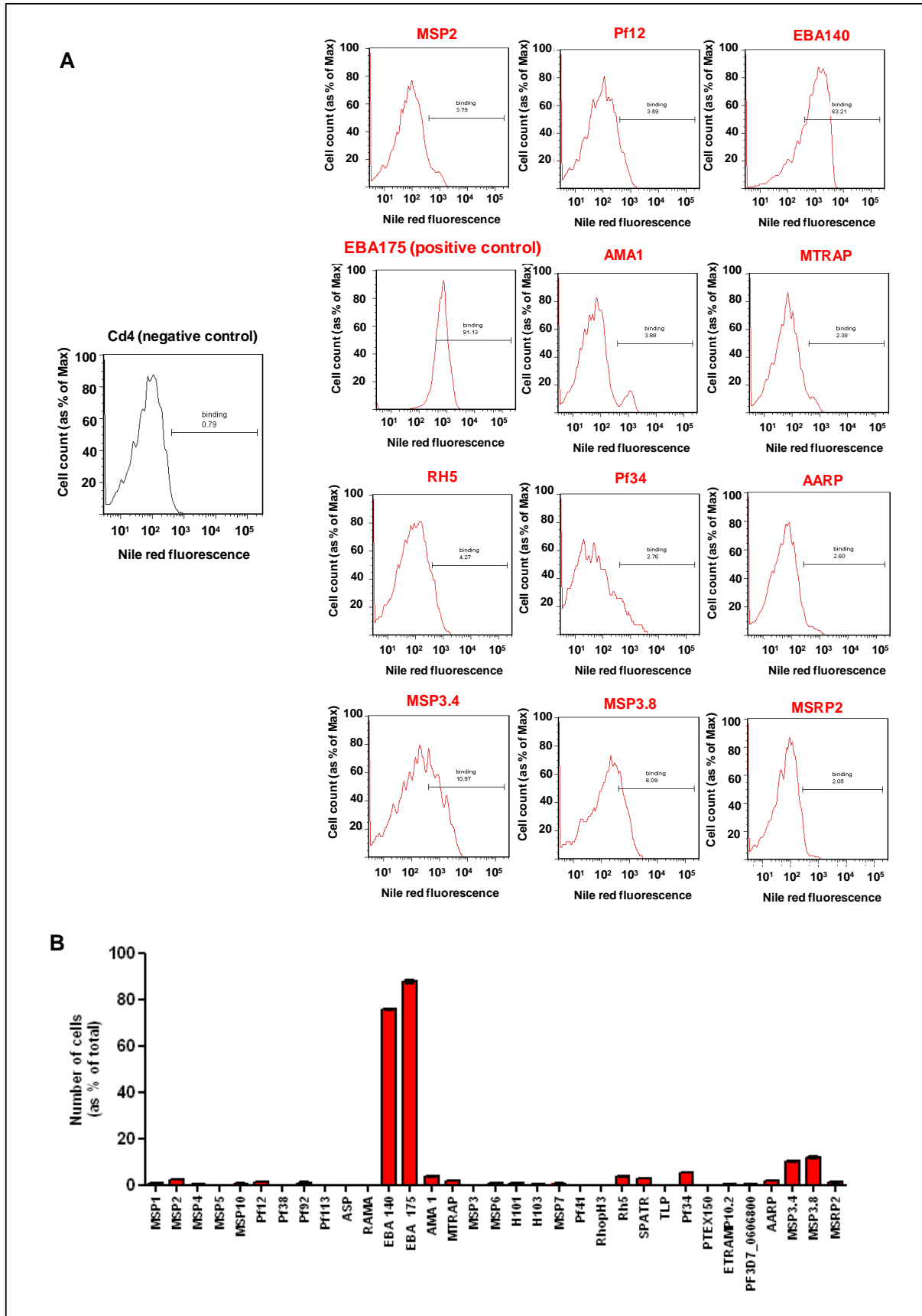


Figure 45. The *P. falciparum* surface proteins, multimerised on fluorescent beads, were presented to human erythrocytes to identify putative interactions. Multimeric arrays of the 33 *P. falciparum* proteins, generated by their immobilisation on streptavidin-coated Nile red beads, were incubated with untreated human erythrocytes for 1 h at 4°C before analysis by flow cytometry. The histograms (**A**) show the fluorescence intensities (at the Nile red emission wavelength) of selected erythrocyte populations each incubated with beads coated with a particular *Plasmodium* protein. The gate marked was used to estimate the number of erythrocytes (as a percentage of total) associated with beads in each case. The calculated values for the entire panel of *P. falciparum* proteins, after subtraction of the background binding (i.e. association with the negative control Cd4-coated beads), are shown in **B**. Each bar indicates mean \pm standard deviation; $n=2$.

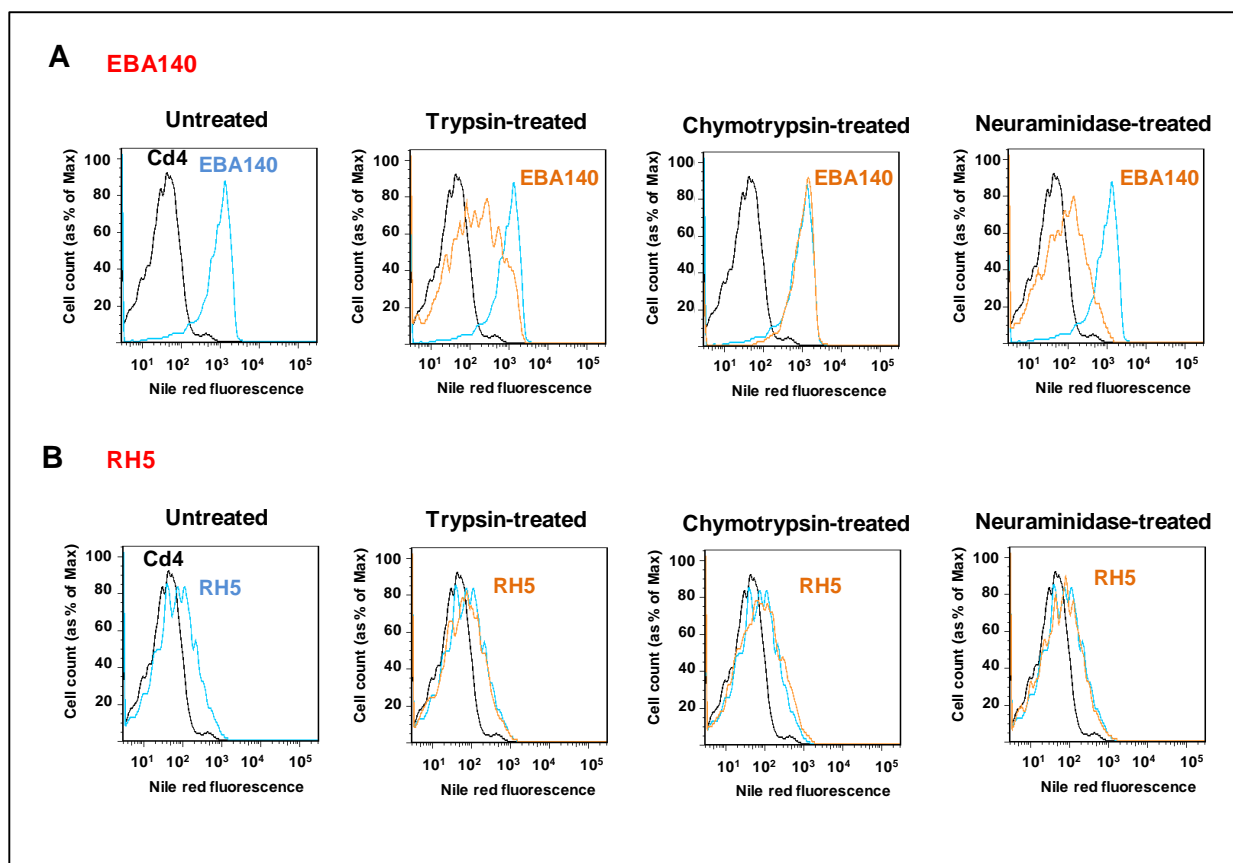


Figure 46. The specificity of the observed binding of EBA140 and RH5 to human erythrocytes was tested by probing these proteins against cells enzymatically pre-treated with trypsin, chymotrypsin and neuraminidase. Nile red beads coated with EBA140 or RH5 were incubated with erythrocytes, which were either untreated (positive control) or pre-treated with the enzymes trypsin (1 mg/ml), chymotrypsin (1 mg/ml) or neuraminidase (100 mU/ml). The histograms show the fluorescence intensities (at the Nile red emission wavelength) of the different erythrocyte populations as estimated by flow cytometry. Untreated erythrocytes incubated with Cd4-coated beads (negative control) are shown in black and those incubated with EBA140 (**A**) or RH5 (**B**) in blue. The enzymatically pre-treated erythrocytes are shown in orange. The results are representative of three independent experiments.

5.2.2 An expression library of erythrocyte multi-pass proteins was compiled based on published literature and protein topology modelling.

Thirty eight multi-pass proteins were chosen for probing against the *P. falciparum* merozoite surface protein library, all of which were identified in a recent mass-spectrometry based comprehensive study of the human erythrocyte proteome (Pasini *et al.*, 2006; Table 7). Many of these receptors have multiple splice-isoforms. For 16 of these, it had not been possible to unequivocally discriminate between the different variants using only the mass-spectrometry data (Pasini *et al.*, 2006; Table 7, Part 2). In these cases, the longest isoform of each receptor was obligatorily selected for inclusion in the screen. The amino acid sequence of each shorter isoform of each receptor was compared to that of its longest isoform by alignment using ClustalW software (Larkin *et al.*, 2007), and if there were no differences in sequence with the exception of deletions, or if the differences lie in predicted intracellular regions, the shorter isoform was not selected for the screen. Selection of variants was based on the assumption that only sequence differences in the extracellular regions of the multi-pass receptors would influence the binding to any *Plasmodium* ligands. There was some difficulty in reaching a consensus regarding the membrane topology of certain proteins, as the predictions on UniProtKB significantly differed from literature sources and/or with the computational predictions from TMpred (Hofmann and Stoffel, 1993), TMHMM 2.0 (Krogh *et al.*, 2003) and HMMTOP 2.0 (Tusnady and Simon, 2001). A total of 41 proteins (including two isoforms each of three receptors) were selected for the screen (Table 7). TrueORF clones (Figure 6) for these proteins were obtained from OriGene and DNA preparations at suitable concentrations for transfection of HEK293E were prepared. TrueORF clones are designed to enable the expression of the encoded proteins with their endogenous signal sequences and C-terminal Myc and DDK tags, in mammalian expression systems (Figure 6). In principle, the recombinant erythrocyte multi-pass receptors should be

Table 7. Erythrocyte multi-pass receptors to be included in the screen.

Part 1: receptors for which a single isoform was unequivocally identified in the mass-spectrometry based study conducted by Pasini *et al.*, 2006.

TMH: transmembrane helices, N-ext: N-terminus is extracellular, N-cyt: N-terminus is intracellular

Protein name (gene name)	NCBI reference sequence numbers		Predicted membrane topology of the protein			
	Protein	mRNA	TMpred	HMMTOP 2.0	TMHMM 2.0	UniProtKB entry
1. Potassium channel subfamily K member 5 (KCNK5)	NP_003731.1	NM_003740.3	7 TMH, N-ext	5 TMH, N-ext	6 TMH, N-ext	4 TMH, N-cyt
2. Secretory carrier-associated membrane protein 4 (SCAMP4)	NP_524558.1	NM_079834.2	3 TMH, N-ext	4 TMH, N-cyt	4 TMH, N-cyt	4 TMH, N-cyt
3. Intermediate conductance calcium-activated potassium channel protein 4 (KCNN4)	NP_002241.1	NM_002250.2	5 TMH, N-ext	7 TMH, N-ext	5 TMH, N-cyt	7 TMH
4. Solute carrier family 12 member 7 (SLC12A7)	NP_006589.2	NM_006598.2	12 TMH, N-cyt	11 TMH, N-cyt	11 TMH, N-cyt	12 TMH, N-cyt
5. Monocarboxylate transporter 1 (SLC16A1)	NP_003042.3	NM_003051.3	10 TMH, N-cyt	12 TMH, N-cyt	11 TMH, N-ext	12 TMH, N-cyt
6. Rhesus blood group-associated glycoprotein (RHAG)	NP_000315.2	NM_000324.2	10TMH, N-cyt	10 TMH, N-ext	11 TMH, N-ext	12 TMH, N-cyt
7. Solute carrier family 2, facilitated glucose transporter member 3 (SLC2A3)	NP_008862.1	NM_006931.2	12 TMH, N-cyt	12 TMH, N-cyt	10 TMH, N-cyt	12 TMH, N-cyt
8. Solute carrier family 2 facilitated glucose transporter member 1 (SLC2A1)	NP_006507.2	NM_006516.2	13 TMH, N-cyt	13 TMH, N-ext	12 TMH, N-cyt	12 TMH, N-cyt
9. Band 3 anion transport protein (SLC4A1)	NP_000333.1	NM_000342.3	11TMH, N-cyt	13 TMH, N-ext	11 TMH, N-ext	12 TMH, N-cyt
10. Fatty acid transporter 4 (SLC27A4)	NP_005085.2	NM_005094.2	5 TMH, N-ext	2 TMH, N-ext	2 TMH, N-ext	2 TMH, N-ext
11. ATP-binding cassette, sub-family G, member 2 (ABCG2)	NP_004818.2	NM_004827.2	6 TMH, N-ext	7 TMH, N-ext	6 TMH, N-ext	6 TMH, N-cyt
12. Vacuolar ATP synthase 16 kDa proteolipid subunit (ATP6V0C)	NP_001685.1	NM_001694.2	4 TMH, N-cyt	4 TMH, N-ext	4 TMH, N-ext	4 TMH, N-cyt
13. Transmembrane protein 222 (TMEM222)	NP_115501.2	NM_032125.2	3 TMH, N-ext	2 TMH, N-cyt	3 TMH, N-ext	3 TMH, N-ext
14. Large neutral amino acids transporter small subunit 4 (SLC43A2)	NP_689559.1	NM_152346.1	12 TMH, N-cyt	12 TMH, N-cyt	12 TMH, N-cyt	12 TMH
15. Glutamate receptor, metabotropic 4 precursor (GRM4)	NP_000832.1	NM_000841.1	9 TMH, N-ext	7 TMH, N-ext	6 TMH, N-ext	7 TMH, N-ext
16. Glutamate transporter (SLC1A7)	NP_006662.3	NM_006671.4	10 TMH, N-ext	11 TMH, N-cyt	7 TMH, N-cyt	10 TMH, N-cyt
17. RECS1 protein homolog (TMBIM1)	NP_071435.2	NM_022152.4	7 TMH, N-cyt	7 TMH, N-ext	7 TMH, N-cyt	7 TMH, N-cyt
18. Aquaporin 1 (Aquaporin-CHIP)(AQP1)	NP_932766.1	NM_198098.1	6 TMH, N-ext	6 TMH, N-cyt	6 TMH, N-cyt	6 TMH, N-cyt
19. Membrane transport protein XK (XK)	NP_066569.1	NM_021083.2	7 TMH, N-cyt	9 TMH, N-ext	9 TMH, N-cyt	10 TMH, N-cyt
20. Iron-regulated transporter, member 1 (SLC40A1)	NP_055400.1	NM_014585.5	9 TMH, N-cyt	11 TMH, N-ext	10 TMH, N-cyt	10 TMH, N-cyt
21. Folate transporter 1 (SLC19A1)	NP_919231.1	NM_194255.1	12 TMH, N-cyt	12 TMH, N-cyt	11 TMH, N-ext	12 TMH, N-cyt
22. Solute carrier family 43, member 1 (SLC43A1)	NP_003618.1	NM_003627.4	12 TMH, N-cyt	12 TMH, N-cyt	12 TMH, N-cyt	12 TMH, N-cyt
23. Sodium/potassium-transporting ATPase alpha-2 (ATP1A2)	NP_000693.1	NM_000702.3	9 TMH, N-cyt	10 TMH, N-cyt	8 TMH, N-cyt	10 TMH, N-cyt
24. Transmembrane protein 56 (TMEM56)	NP_689700.1	NM_152487.2	6 TMH, N-cyt	6 TMH, N-cyt	6 TMH, N-cyt	6 TMH

Table 7. Erythrocyte multi-pass receptors to be included in the screen.

Part 2: receptors for which a single isoform was not unequivocally identified in the mass-spectrometry based study conducted by Pasini *et al.*, 2006.

TMH: transmembrane helices, N-ext: N-terminus is extracellular, N-cyt: N-terminus is intracellular

Protein name (gene name)	NCBI reference sequence numbers		Predicted membrane topology of the protein			
	Protein	mRNA	TMpred	HMMTOP 2.0	TMHMM 2.0	UniProtKB entry
25. Solute carrier family 43 member 3 (SLC43A3)	NP_054815.2	NM_014096.2	11 TMH, N-ext	11 TMH, N-ext	11 TMH, N-ext	12 TMH, N-cyt
26. Na/K-transporting ATPase alpha-1 (ATP1A1)	NP_001153705.1	NM_001160233.1	9 TMH, N-cyt	10 TMH, N-cyt	8 TMH, N-cyt	10 TMH, N-cyt
27. Plasma membrane calcium-transporting ATPase 4 (ATP2B4)	NP_001675.3	NM_001684.3	10 TMH, N-cyt	10 TMH, N-cyt	8 TMH, N-cyt	10 TMH, N-cyt
28. Ion transporter protein (SLC22A23)	NP_056297.1	NM_015482.1	13 TMH, N-ext	12 TMH, N-cyt	10 TMH, N-cyt	10 TMH, N-ext
29. Equilibrative nucleoside transporter 1 (SLC29A1)	NP_001071645.1	NM_001078177.1	11 TMH, N-ext	11 TMH, N-cyt	11 TMH, N-cyt	11 TMH, N-cyt
30. Leukocyte surface antigen CD47 precursor (CD47)	NP_001768.1	NM_001777.3	5 TMH, N-ext	5 TMH, N-ext	6 TMH, N-cyt	5 TMH, N-ext
31. Thyrotropin receptor precursor (TSHR)	NP_000360.2	NM_000369.2	7 TMH, N-ext	7 TMH, N-ext	7 TMH, N-cyt	7 TMH, N-ext
32. Urea transporter (SLC14A1)	NP_001122060.3	NM_001128588.3	8 TMH, N-cyt	10 TMH, N-cyt	8 TMH, N-cyt	9 TMH, N-cyt
33. Multidrug resistance-associated protein 1 (ABCC1)	NP_004987.2	NM_004996.3	17 TMH, N-ext	16 TMH, N-ext	16 TMH, N-ext	17 TMH, N-ext
34. Multidrug resistance-associated protein 4 (ABCC4)	NP_005836.2	NM_005845.3	10 TMH, N-cyt	10 TMH, N-ext	11 TMH, N-cyt	14 TMH, N-cyt
35. Tetraspanin-14 (TSPAN14)	NP_112189.2	NM_030927.2	4 TMH, N-cyt	4 TMH, N-cyt	4 TMH, N-cyt	4 TMH, N-cyt
36 and 37. Cytochrome b reductase 1 (CYBRD1)	NP_079119.3	NM_024843.3	6 TMH, N-ext	6 TMH, N-cyt	6 TMH, N-cyt	6 TMH, N-cyt
	NP_001120855.1	NM_001127383.1	2 TMH, N-ext	2 TMH, N-ext	2 TMH, N-cyt	
38 and 39. Duffy antigen/chemokine receptor (DARC)	NP_001116423.1	NM_001122951.1	7 TMH, N-ext	7 TMH, N-ext	7 TMH, N-ext	7 TMH, N-ext
	NP_002027.2	NM_002036.2	7 TMH, N-ext	7 TMH, N-ext	7 TMH, N-cyt	
40 and 41. Rh blood CE group antigen polypeptide (RHCE)	NP_065231.2	NM_020485.3	10 TMH, N-cyt	12 TMH, N-cyt	12 TMH, N-cyt	11 TMH
	NP_619524.2	NM_138618.2	8 TMH, N-cyt	9 TMH, N-cyt	9 TMH, N-cyt	

successfully expressed and targeted to the cell surface in HEK293E; they are expressed in a human cell line (hence problems with codon usage and post-translational modifications should not be encountered), they carry their endogenous signal sequences (which would direct them to the surface membrane) and the C-terminal Myc and DDK tags are unlikely to interfere with the correct folding of the protein, due to their small size. To confirm this, the expression in HEK293E and trafficking to the surface membrane of a few of the proteins, were monitored over a period of 72 hours after transfection, by staining cells with appropriate antibodies and using flow cytometry. The longest isoform of the Duffy antigen (gene name DARC) was detected using a goat polyclonal antibody against its N-terminal ectodomain and a FITC-conjugated anti-goat antibody on non-permeabilised cells (Figure 47 A). The results suggest that this Duffy isoform was displayed on the surface of transfected cells in the correct orientation (i.e. with the N-terminus exposed at the extracellular face of the membrane). This was also confirmed by analysis of the antibody-stained cells using confocal microscopy (Figure 47 B). The flow cytometry data also suggests that the amount of recombinant Duffy at the cell surface was highest 48 hours after transfection (Figure 47 A). The RECS1 protein homolog (TMBIM1) and isoform 2 of cytochrome b reductase 1 (CYBRD1) were also detected on the surface of transfected non-permeabilised HEK293E cells using a mouse monoclonal antibody against the c-Myc fusion tag and a FITC-conjugated anti-mouse secondary (Figure 47 C and D). These proteins also showed the highest expression 48 h after transfection.

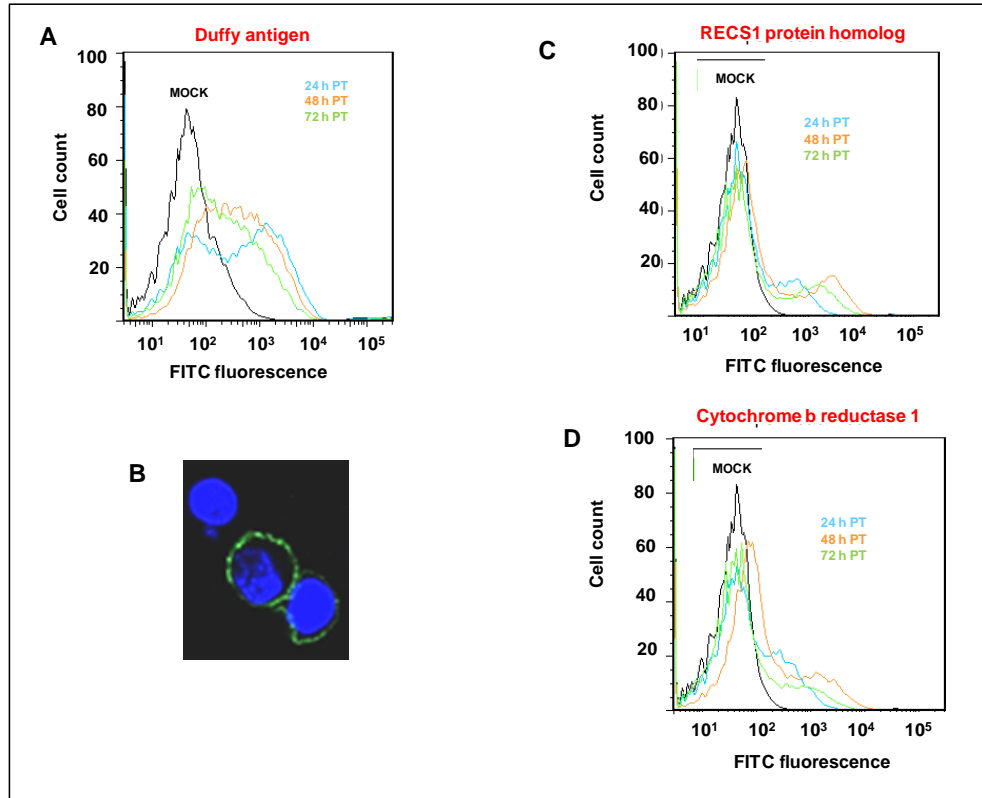


Figure 47. The expression of three recombinant multi-pass receptors on the surface of HEK293E cells was tracked after transient transfection of their expression constructs over a period of 72 h. The TrueORF clones of the long isoforms of the Duffy antigen and Cytochrome b reductase 1 as well as the RECS1 protein homolog were transiently transfected into HEK293E cells. The expression of the receptors and their display at the surface of transfected cells was monitored ~ every 24 h for 3 days. The Duffy antigen was detected using a goat polyclonal against its N-terminal extracellular domain and a FITC-conjugated donkey anti-goat secondary. The other two receptors are predicted to have C-terminal extracellular domains and hence were detected using a mouse monoclonal against their c-Myc tag and a FITC-conjugated rabbit anti-mouse secondary. Mock-transfected cells (treated only with the transfection reagent) stained with the same antibodies were used as a negative control in each case. The expression of the Duffy antigen was analysed both by flow cytometry (A) and confocal microscopy (B). In the confocal microscope image (taken 48 h after transfection), DAPI staining of the cell nuclei is shown in blue and FITC staining in green. The expression of the RECS1 protein homolog (C) and Cytochrome b reductase 1 (D) was analysed only by flow cytometry.

5.2.3 Proof-of-principle study: demonstration of the interaction between Cd200 and its receptor with one partner expressed transiently on the surface of HEK293E cells and the other immobilised on fluorescent beads.

A proof-of-principle study was performed to assess the technical feasibility and efficiency of detecting a low-affinity interaction between a protein expressed on the surface of HEK293E cells by transient transfection and another immobilised on fluorescent beads, using flow cytometry. The well characterised interaction ($K_D = 2.5 \mu\text{M}$) between the single-pass transmembrane proteins, rat Cd200 protein and its structurally related receptor (Cd200R) was selected for this purpose (Preston et al., 1997; Wright *et al.*, 2000; Wright *et al.*, 2003). In the first instance, Cd200 with a C-terminal EGFP tag was expressed on the surface of HEK293E cells by transient transfection and incubated with Nile red beads coated with biotinylated Cd4, Cd200 or Cd200R. Almost all of the transfected cells (EGFP+) were observed to bind to Cd200R-coated beads but not to beads coated with Cd4 or Cd200 (Figure 48 A). When the experiment was repeated in the reciprocal orientation with EGFP-tagged Cd200R expressed on the surface of HEK293E cells, the EGFP+ cells were also observed to bind only to Cd200-coated beads (Figure 48 A). The specificity of the observed interaction between Cd200 and Cd200R was probed further by pre-incubating the Cd200-expressing cells with an anti-Cd200 mouse monoclonal antibody, OX2 and an isotype-matched negative control antibody, W6/32. Pre-treatment of cells with OX2 but not W6/32, was observed to completely block the interaction with Cd200R-coated beads (Figure 48 B). Overall, the results from the proof-of-principle study suggest that this experimental method is of high efficiency and specificity.

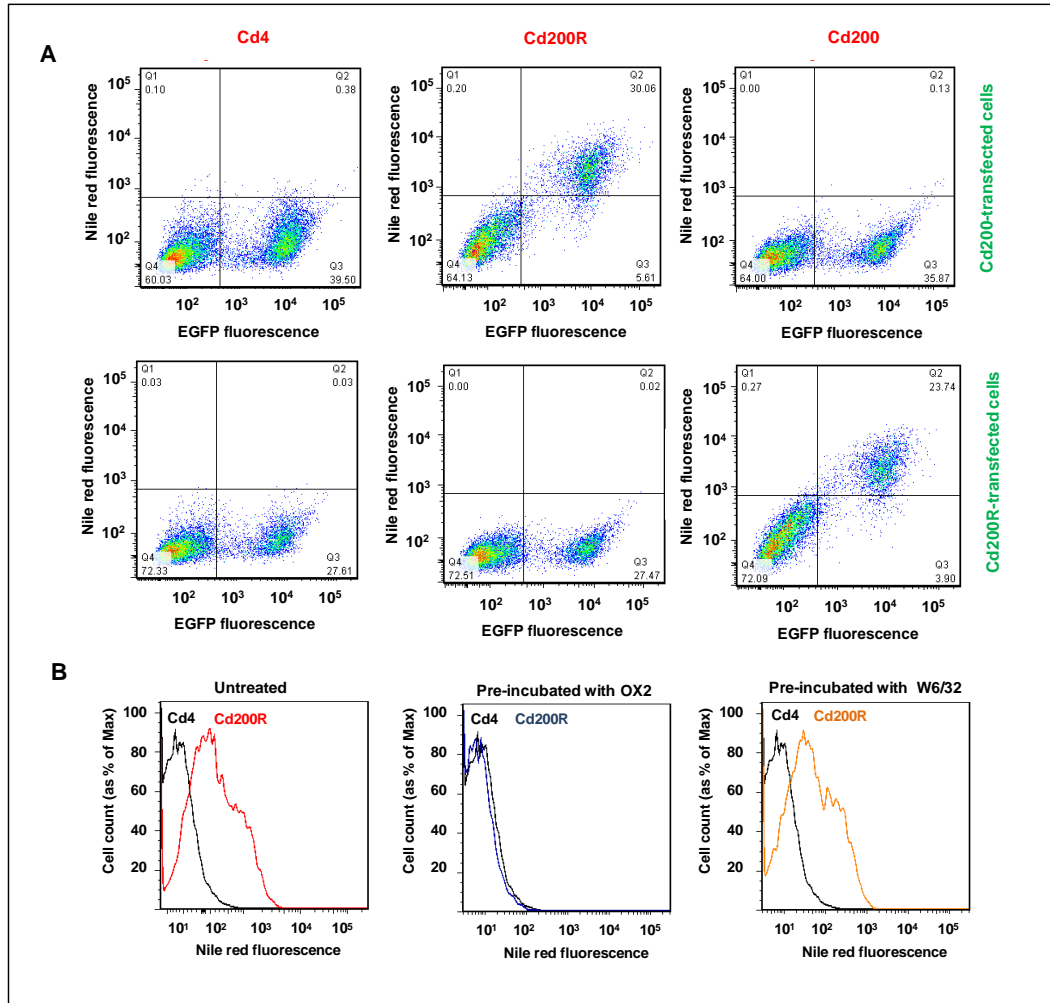


Figure 48. A ‘proof-of-principle’ study: The low-affinity interaction between the single-pass membrane proteins Cd200 and its structurally similar receptor (Cd200R) could be detected when one partner was expressed transiently on the surface of HEK293E cells and the ectodomain of the other immobilised on fluorescent beads. HEK293E cells were transiently transfected with the expression construct for cytosolic C-terminal EGFP-tagged Cd200 or Cd200R and then presented with Nile red beads coated with the biotinylated ectodomains of Cd200, Cd200R or Cd4. Binding events were detected by flow cytometry. **A)** Dot plots, of EGFP *versus* Nile red fluorescence, of transfected HEK293E cells incubated with the protein-coated beads. **B)** Histograms of the fluorescence intensity, at the Nile red emission wavelength, of Cd200-expressing HEK293E cells that were either untreated or pre-treated with specific mouse monoclonals, prior to incubation with Cd200R- and Cd4-coated beads. OX2: anti-Cd200 antibody, W6/32: isotype-matched negative control antibody. Both antibodies were used at $0.5 \mu\text{g}/10^6$ cells.

5.2.4 Positive control study: demonstration of the interaction between the Duffy antigen expressed recombinantly on the surface of HEK293E cells by transient transfection and PvDBP immobilised on fluorescent beads.

The interaction between the Duffy antigen and PvDBP was selected as a positive control to confirm the ability to detect low affinity binding of a multi-pass receptor transiently-expressed on the surface of HEK293E cells and a recombinant *Plasmodium* protein immobilised on fluorescent beads.

The full-length ectodomain of PvDBP (PvDBP FL) was produced in recombinant, soluble form with C-terminal Cd4 and biotin tags. The expression of the protein at the expected size of 136 kDa was confirmed by Western blotting and ELISA assays were used to monitor the process of immobilising this protein on streptavidin-coated Nile red beads (Figure 49 A and B). When presented to erythrocytes, PvDBP FL-coated beads showed higher binding relative to the negative control (Cd4-coated beads) (Figure 49 C).

Two isoforms of the Duffy antigen have been identified, which differ only at the very beginning of the N-terminal extracellular domain. The major isoform is shorter than the minor by two residues and also differs in the identity of six residues. These differences reside outside of, but adjacent to, the putative PvDBP binding region (Figure 49 D). The TrueORF clones of both Duffy isoforms were transiently-transfected in HEK293E cells and expression was monitored 48 h subsequently using the anti-DARC rabbit polyclonal raised against the N-terminal extracellular domain and a FITC-conjugated anti-rabbit secondary (Figure 49 E and F). In comparison to the secondary only control, some staining of mock-transfected cells (treated only with the transfection reagent) was observed, suggesting some basal-level of Duffy expression on HEK293E cells. Cells transfected with the expression constructs of the recombinant Duffy isoforms however, showed much higher binding to the anti-DARC antibody than mock-

transfected cells (the median fluorescence intensity of these cells was about 10-fold higher), suggesting that these recombinant proteins were present in the correct orientation at the cell surface. The expression levels of the two isoforms were fairly similar, with the shorter isoform being expressed slightly more.

Mock-transfected cells and those putatively expressing the two isoforms of Duffy were then tested against *Pv*DBP FL-coated beads (Figure 49 G, H and I). In comparison to Cd4-coated beads, binding of *Pv*DBP FL-coated beads was observed to mock-transfected cells as well as to those expressing recombinant Duffy (Figure 49 G). Direct comparison of *Pv*DBP binding to the different cell populations revealed significantly higher binding to cells over-expressing the short isoform of Duffy relative to mock-transfected cells (Figure 49 H and I). The binding of *Pv*DBP to cells expressing the long Duffy isoform was slightly less than the binding to mock-transfected cells. One possible explanation for these results is that only the short isoform of Duffy is capable of binding to *Pv*DBP and that HEK293E cells normally express a basal-level of this isoform endogenously. Therefore, only over-expression of the short isoform of Duffy and not the long would lead to higher binding to *Pv*DBP above the background binding observed with mock-transfected cells.

5.2.5 More than 40% of *P. falciparum* merozoite surface proteins tested showed binding to untreated and mock-transfected HEK293E cells.

Prior to screening the *P. falciparum* merozoite surface protein library against the panel of erythrocyte multi-pass receptors, the binding of the parasite proteins to untreated and mock-transfected HEK293E cells was tested (Figure 50). As HEK293E cells were to be used as the expression host for the recombinant multi-pass receptors, it was important to have an understanding of the background level of binding shown by each *P. falciparum* protein to

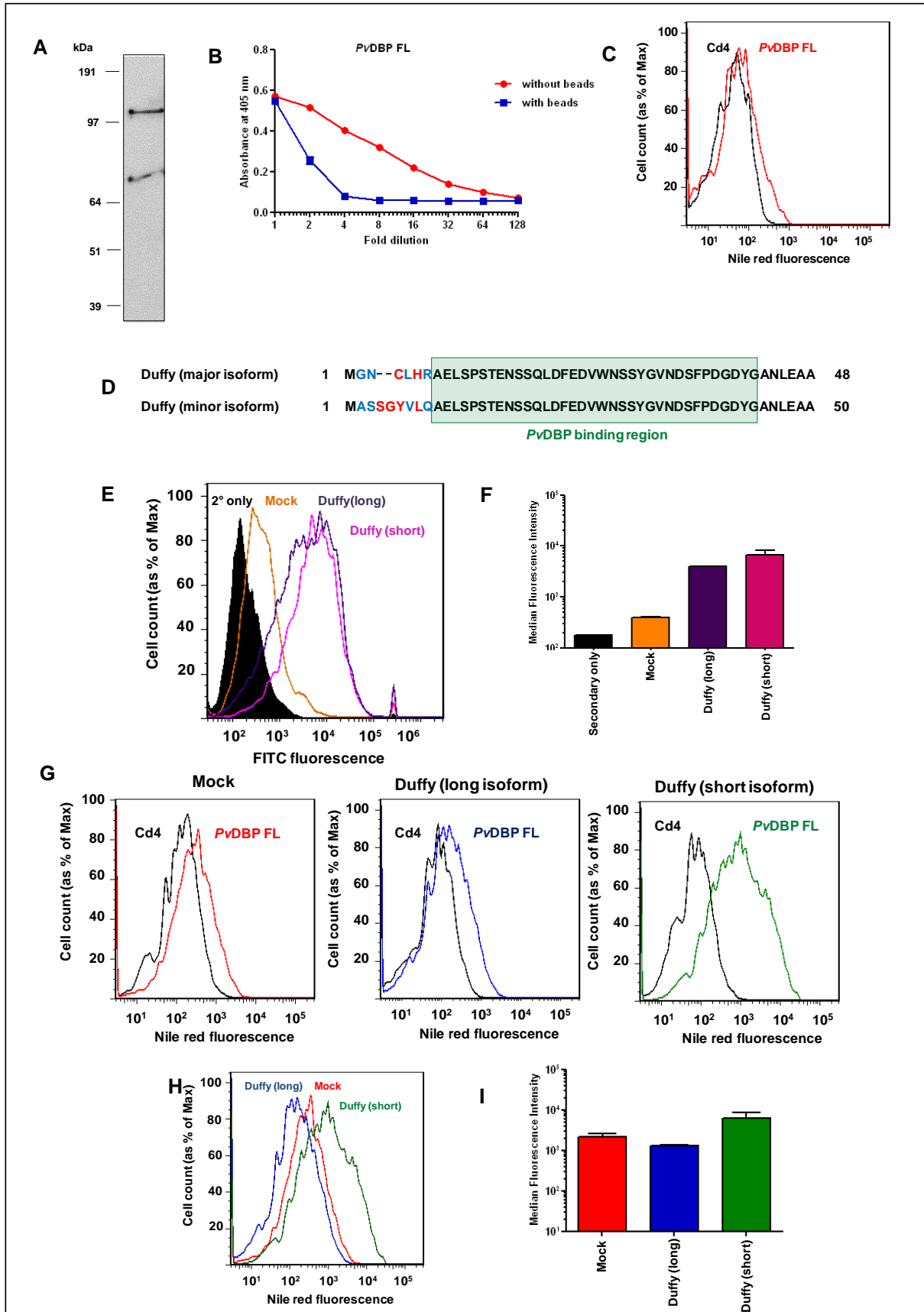


Figure 49. A “positive control” study: The Duffy antigen, a multi-pass receptor, expressed on the surface of HEK293E cells, showed binding to its known ligand, *P. vivax* DBP (*Pv*DBP) immobilised on fluorescent beads. The full-length ectodomain of *Pv*DBP (*Pv*DBP FL, protein accession number: P22290, residues 21-1070) was expressed with C-terminal Cd4 and biotin tags. Multimeric arrays of the protein were generated by direct attachment to streptavidin-coated Nile red beads. *Pv*DBP FL-coated beads were presented first to human erythrocytes to confirm functional activity and then to HEK293E cells transiently transfected with the TrueORF clones of the Duffy isoforms. The expression of the Duffy isoforms and the binding of *Pv*DBP FL-coated beads to cells were detected by flow cytometry. **A)** Western blot of *Pv*DBP FL (136 kDa), performed using extravidin-HRP as the probe. **B)** The minimum amount of *Pv*DBP FL necessary for complete saturation of a set number of streptavidin-coated Nile red beads was determined by ELISA, as described before. Data are shown as mean \pm standard deviation; $n=3$. **C)** Histograms of Nile red fluorescence *versus* cell count, of erythrocyte populations incubated with *Pv*DBP FL-coated beads (red) or Cd4-coated beads (black, negative control). The data are representative of two independent experiments. **D)** The N-terminal sequences of the two isoforms of Duffy. Identical and similar residues are shown in black and blue respectively. The *Pv*DBP binding region (residues 8-42) is highlighted in green (Chitnis *et al.*, 1996). **E)** Histograms of HEK293E cells, stained with an anti-Duffy goat polyclonal (directed against the N-terminal extracellular domain) and a FITC-conjugated anti-goat secondary. Mock-transfected cells are shown in orange. HEK293E cells transiently transfected with the Duffy isoforms are represented in purple (long isoform) and pink (short isoform) respectively. Cells stained with only the secondary antibody (negative control) are shown in black. **F)** A bar chart of the median fluorescence intensities (at the FITC emission wavelength) of the antibody-stained HEK293E cells. Data are shown as mean \pm standard deviation; $n=2$. **G)** and **H)** Histograms showing the fluorescence intensities of HEK293E cells incubated with *Pv*DBP FL-coated Nile red beads. Red: mock-transfected cells, blue: cells transfected with the long isoform of Duffy, green: cells transfected with the short isoform of Duffy. The black histograms show the background fluorescence of the cells (i.e. when incubated with Cd4-coated beads). **I)** The bar chart shows the median fluorescence intensities of the different cell populations incubated with *Pv*DBP FL-coated beads. Each bar represents mean \pm standard deviation; $n=2$.

endogenously expressed receptors on the HEK293E cell surface. The assays were performed with Nile red beads coated with the *Plasmodium* proteins and binding events were detected using flow cytometry. As before the number of cells (as a percentage of total) binding to each protein was calculated based on a fluorescence intensity threshold, set with reference to the binding to Cd4-coated beads (negative control) (Figure 50 A). Of the 33 *P. falciparum* proteins tested against untreated and mock-transfected HEK293E cells, 15 showed some degree of binding to both (Figures 50 B and C). Several of the proteins, including AARP, MSRP2 and RhopH3 showed higher binding to mock-transfected cells than to untreated cells suggesting some influence of the transfection reagent on the expression profile of their putative receptors. To confirm the specificity of the observed interactions, selected *Plasmodium* proteins were tested against HEK293E cells pre-treated with neuraminidase (Figure 51). Of the 11 proteins chosen for this analysis, nine had previously been observed to bind to human erythrocytes, the two exceptions were Pf113 and RhopH3. The binding of EBA175, EBA140, Pf113 and MSRP2 were observed to be susceptible to neuraminidase treatment, suggesting the involvement of sialic acid in their recognition of putative receptors on the surface of HEK293E cells (Figure 51). The binding of the other seven proteins, including RH5, was not inhibited by neuraminidase treatment. The gene expression profile of HEK cells, originally generated by adenoviral transformation of human embryonic kidney cells, is not generally considered to be representative of any particular human tissue type (Graham *et al.*, 1977). Therefore, even proteins which are restricted to erythrocytic expression, could in theory be endogenously expressed in HEK293E cells. To test this hypothesis, HEK293E cells were stained with two mouse monoclonal antibodies, BRIC256 and MEM-M6/6, which recognise Glycophorin A and BSG respectively (Figure 52). The staining was detected using a FITC-conjugated anti-mouse secondary.

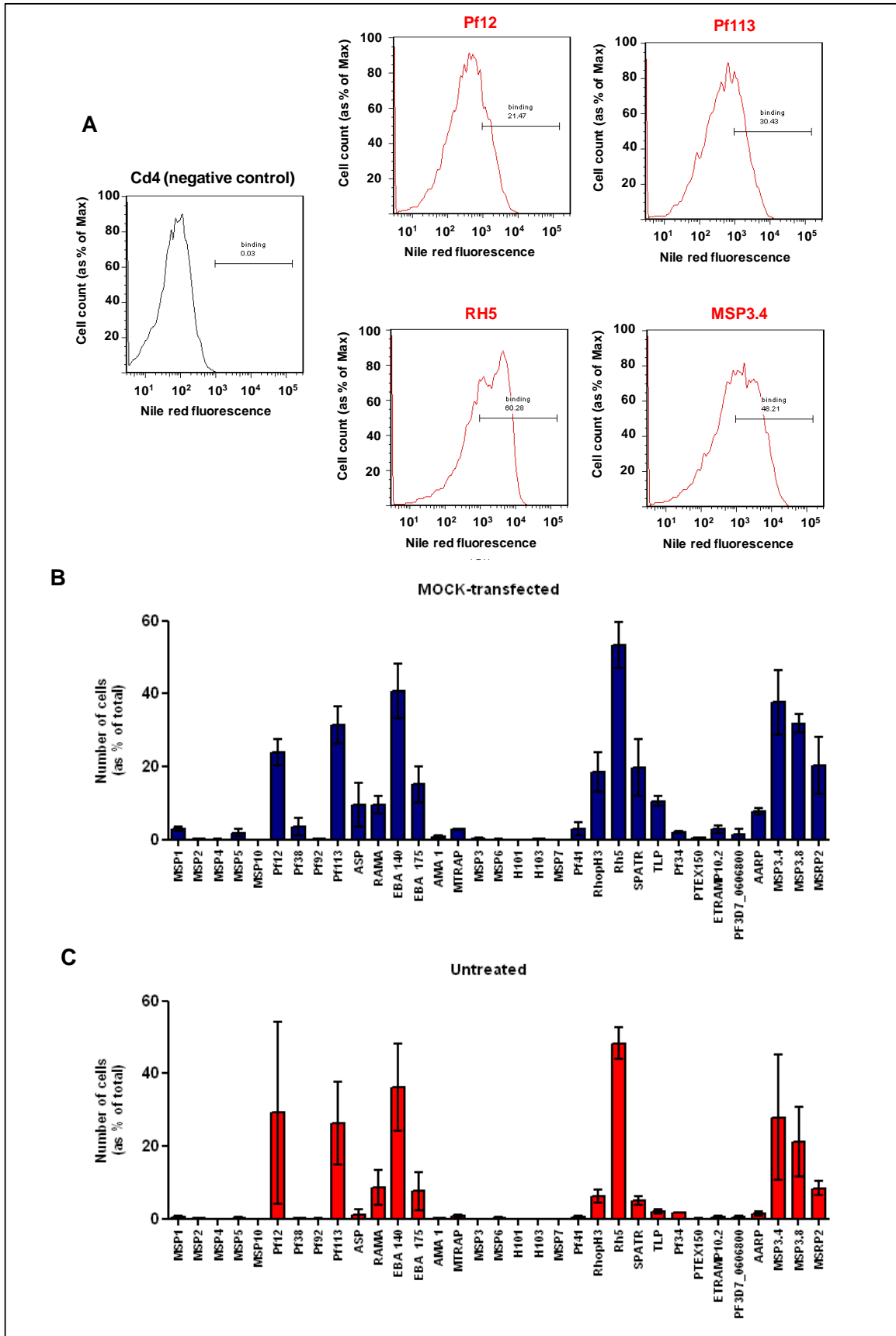


Figure 50. A significant proportion of the *P. falciparum* surface proteins tested showed some binding to untreated and mock-transfected HEK293E cells. Multimeric arrays of the 33 *P. falciparum* proteins, generated by immobilising the proteins on streptavidin-coated Nile red beads, were incubated with untreated and mock-transfected HEK293E cells before analysis by flow cytometry. The histograms (A) show the fluorescence intensities (at the Nile red emission wavelength) of selected cell populations each incubated with beads coated with a specific *Plasmodium* protein. The gate marked was used to estimate the number of cells (as a percentage of total) associated with beads in each case. The calculated values for the entire panel of *P. falciparum* proteins, after subtraction of the background binding (i.e. association with the negative control Cd4-coated beads), are shown in B and C. Each bar indicates mean \pm standard deviation; $n=3$.

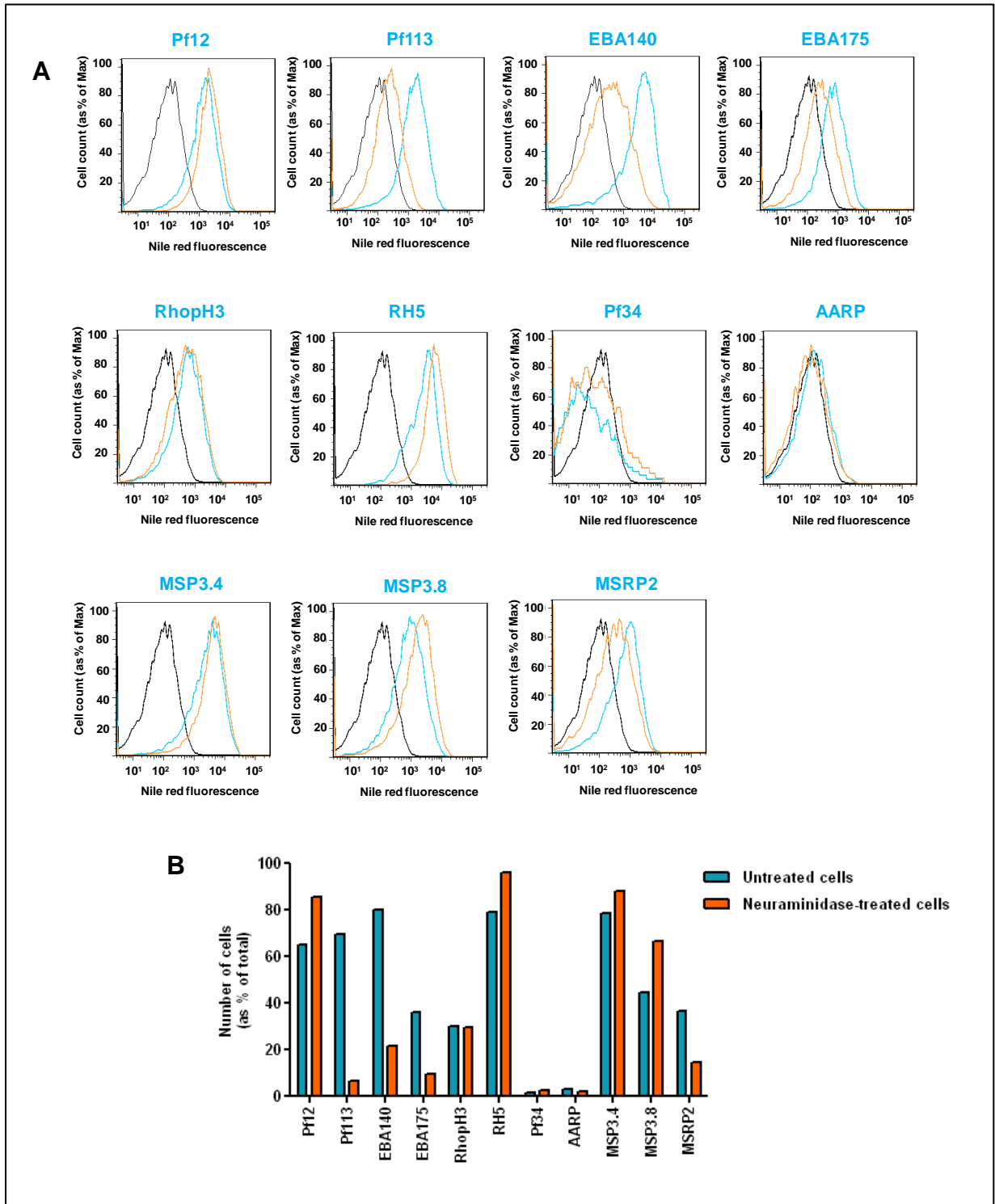


Figure 51. Four out of 11 *P. falciparum* proteins tested showed sialic-acid dependent binding to HEK293E cells. 11 of the *Plasmodium* proteins (immobilised on Nile red beads) were tested for binding to HEK293E cells pre-treated with neuraminidase (100 mU/ml). Untreated cells were included as a positive control. **A)** The histograms show the fluorescence intensities (at the Nile red emission wavelength) of cells incubated with each *Plasmodium* protein. Untreated cells are shown in blue and neuraminidase-treated cells in orange. The background fluorescence of the cells (i.e. the binding to Cd4-coated beads) is indicated in black. **B)** The bar chart represents the number of untreated and neuraminidase-treated cells (as a percentage of total) binding to each parasite protein, as calculated from the histograms above, using a fluorescence intensity threshold to select the Nile red 'positive' cells.

The average median fluorescence intensities (MFI) of the cells stained with BRIC256 and MEM-M6/6 were 102.2 and 5920.6 respectively, whereas those stained only with the secondary antibody had an average MFI of 75.03. Therefore BSG, the RH5 receptor, clearly appears to be expressed on HEK293E cells at possibly a higher level than observed on human erythrocytes. Some basal degree of Glycophorin A expression on HEK293E cells also seems probable and would account for the relatively low level EBA175 binding observed.

5.2.6 The *P. falciparum* merozoite surface proteins were screened against 41 erythrocytic multi-pass receptors, each expressed individually on the surface of HEK293E cells.

For screening against the *P. falciparum* merozoite surface proteins, the erythrocytic multi-pass receptors were expressed individually on the surface of HEK293E cells by transient transfection of their TrueORF clones. The expression of each receptor was tested by staining non-permeabilised cells with an anti-c-Myc mouse monoclonal and a FITC-conjugated secondary antibody. The multi-pass receptors exhibited a range of expression levels (Figure 53). In some cases (e.g. the Glutamate transporter (SLC1A7)) almost no expression of the protein was detected. However, this could be due to the proteins being oriented at the cell surface with the C-terminus on the cytosolic side. The c-Myc tag in such cases would not be accessible to the antibody.

In the screen, the multi-pass receptors were transfected and tested against the *Plasmodium* proteins in four batches of ten, for ease of handling. Mock-transfected cells were included as a negative control in each batch to account for batch-to-batch variation in the expression levels of cell surface proteins that arise independently of the exogenously-transfected DNA.

In the case of each *Plasmodium* protein, the observed (background) binding to mock-transfected cells was subtracted from the binding to cells transfected with each multi-pass receptor, during

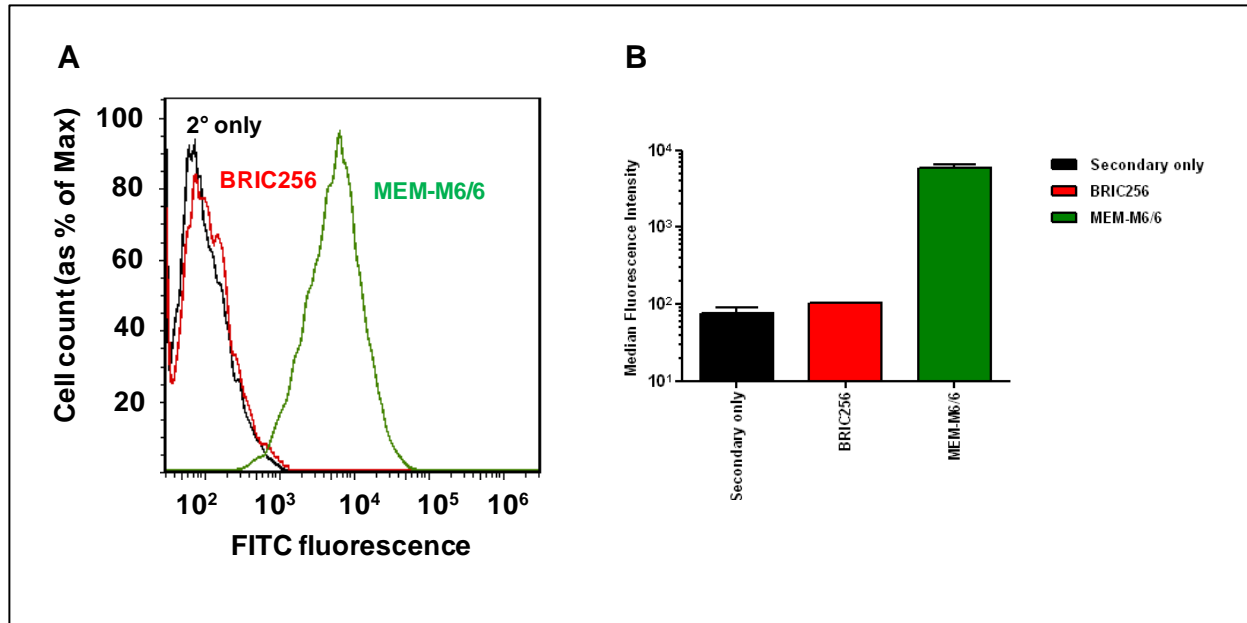


Figure 52. The expression of Glycophorin A and Basigin on the surface of HEK293E cells was tested by staining with specific antibodies. Untreated HEK293E cells were stained with the mouse monoclonals BRIC256 and MEM-M6/6, which recognise Glycophorin A and Basigin respectively. The binding of the monoclonals to the cells was detected with a FITC-conjugated anti-mouse secondary. The cells were also stained with only the secondary as a negative control. **A)** Histograms of fluorescence intensity *versus* cell count of the antibody-stained cells. **B)** A bar chart of the median fluorescence intensities (at the FITC emission wavelength) of the antibody-stained cells. Each bar represents mean \pm standard deviation; $n=2$. Cells stained with BRIC256, MEM-M6/6 and only the secondary are shown in red, green and black respectively.

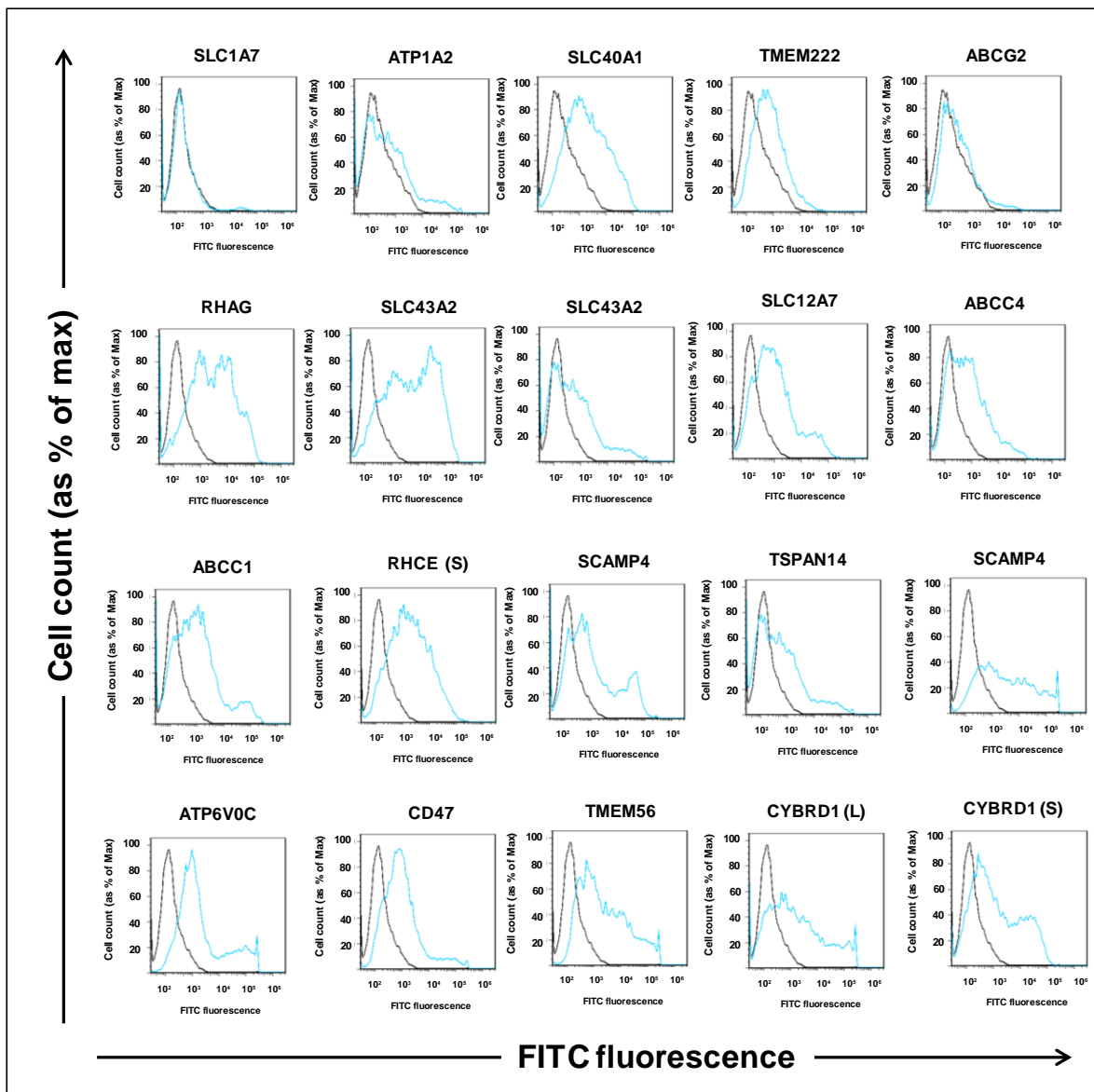


Figure 53. The expression of the recombinant multi-pass receptors on the surface of HEK293E cells was tested by staining with a mouse monoclonal antibody that recognises their C-terminal Myc tag. The cells were analysed 48h after transfection of the TrueORF clones coding for the multi-pass receptors. The binding of the anti-c-Myc monoclonal was detected with a FITC-conjugated anti-mouse secondary using flow cytometry. Mock-transfected cells stained with the same antibodies were used as a negative control. The histograms displayed show the fluorescence intensities (at the FITC emission wavelength) of cells transfected with each stated multi-pass receptor (blue) and mock-transfected cells (black). The multi-pass receptors are referred to by their gene names and the expression profiles of only 20 randomly selected receptors are shown.

data analysis, to estimate the 'actual' binding to the recombinant multi-pass receptor. The values obtained were then normalised (by calculating the z scores) across the whole panel of multi-pass receptors, to identify the most significant interactions more easily. This simple model used for evaluating the data, assumes that any increase seen in the binding of a parasite protein to cells transfected with a recombinant receptor, relative to mock-transfected cells, is the result only of the expression of the receptor and not due to indirect effects of the exogenous DNA.

All the interactions tested in the screen and their estimated z scores are shown (Figure 54). Overall, only two interactions had z scores of above 5, the binding of the *P. falciparum* protein AARP to the Fatty acid transporter 4 (gene name: SLC27A4) and the binding of MSP11 to the Plasma membrane calcium transporting ATPase 4 (ATP2B4) (Figure 55). A z score of 5 means that the binding of the parasite protein to the multi-pass receptor was five standard deviations above the average binding of that *Plasmodium* protein to the entire panel of multi-pass receptors and thus can be considered as an indication of a fairly robust interaction. 11 of the tested interactions had a z scores between 3 and 5 (Figures 56 and 57). These include the interaction of the *P. falciparum* protein H101 with the Plasma membrane calcium transporting ATPase 4 (ATP2B4). Both H101 and MSP11 are members of the MSP3 family of proteins, hence their putative binding to the same receptor seems promising (Figure 56 A). MSP6 was also observed to bind to the Fatty acid transporter 4 (SLC27A4) (Figure 56 B). MSP2 showed binding to two multi-pass receptors; the short isoform of the Rh blood CE group antigen polypeptide (RHCE) and the Monocarboxylate transporter 1 (SLC16A1) (Figure 56 C and D). The interactions of the *Plasmodium* proteins MSP3, MSP4, MSP7 and AMA 1 with the multi-pass receptors Na⁺/K⁺ transporting ATPase (ATP1A1), Multidrug resistance associated protein (ABCC4), Rhesus

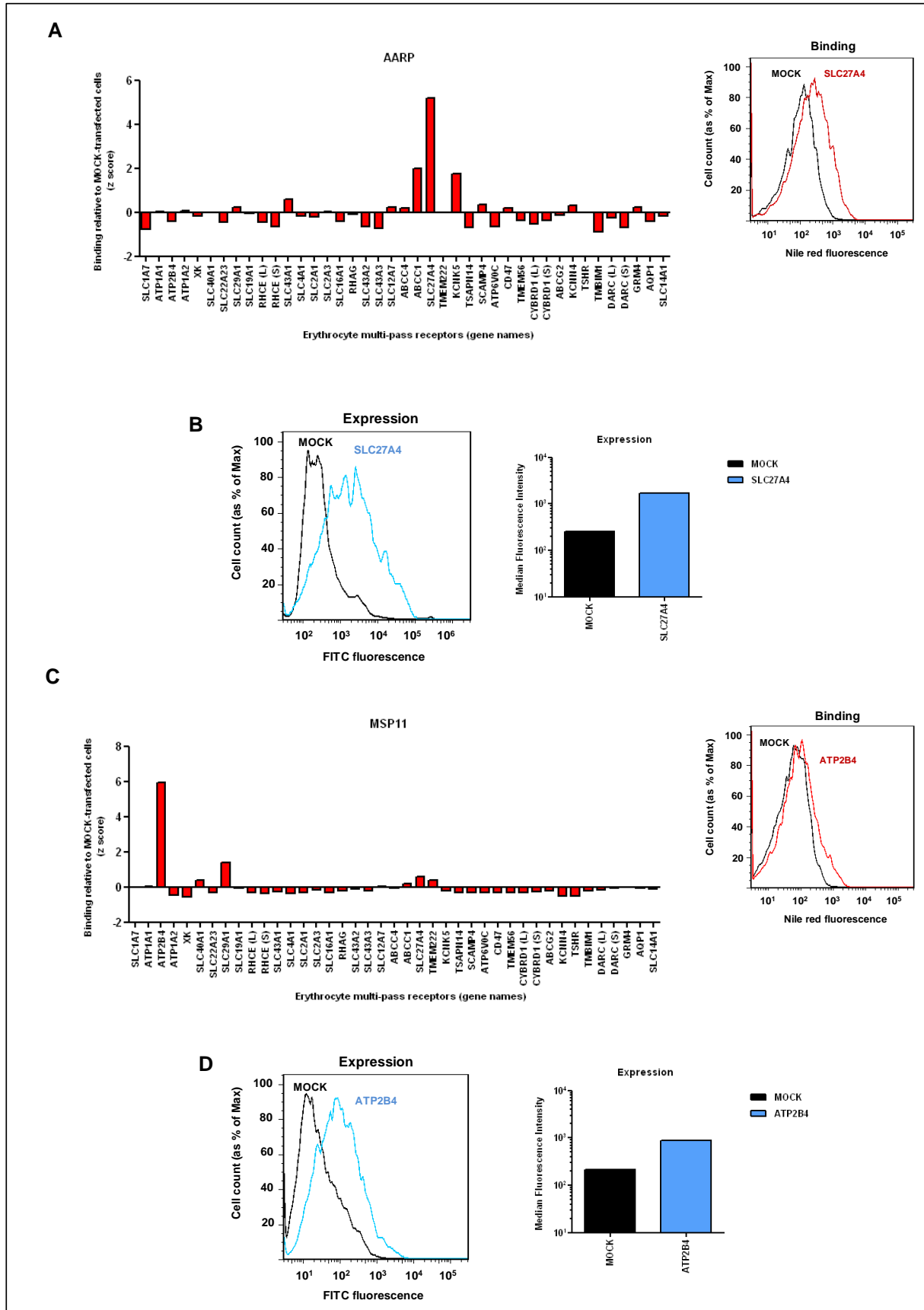


Figure 55. The interactions between the *P. falciparum* proteins AARP and MSP11 with the multi-pass receptors encoded by SLC27A4 (the Fatty acid transporter) and ATP2B4 (Plasma membrane calcium transporting ATPase 4) respectively, were the most significant, with z scores of above 5. A) and C) The bar charts show the normalised binding (z scores) of AARP (A) and MSP11 (C) to the panel of erythrocyte multi-pass receptors. The histograms represent mock-transfected cells (black) and cells transfected with SLC27A4 (red) (A) or ATP2B4 (red) (C), after incubation with AARP-coated Nile red beads. B) and D) The histograms are of mock-transfected cells (black) and cells transfected with SLC27A4 (blue) (B) or ATP2B4 (blue) (D), stained with an anti-c-Myc mouse monoclonal and a FITC-conjugated anti-mouse secondary. The bar charts show the median fluorescence intensities (at the FITC emission wavelength) of the antibody stained cells.

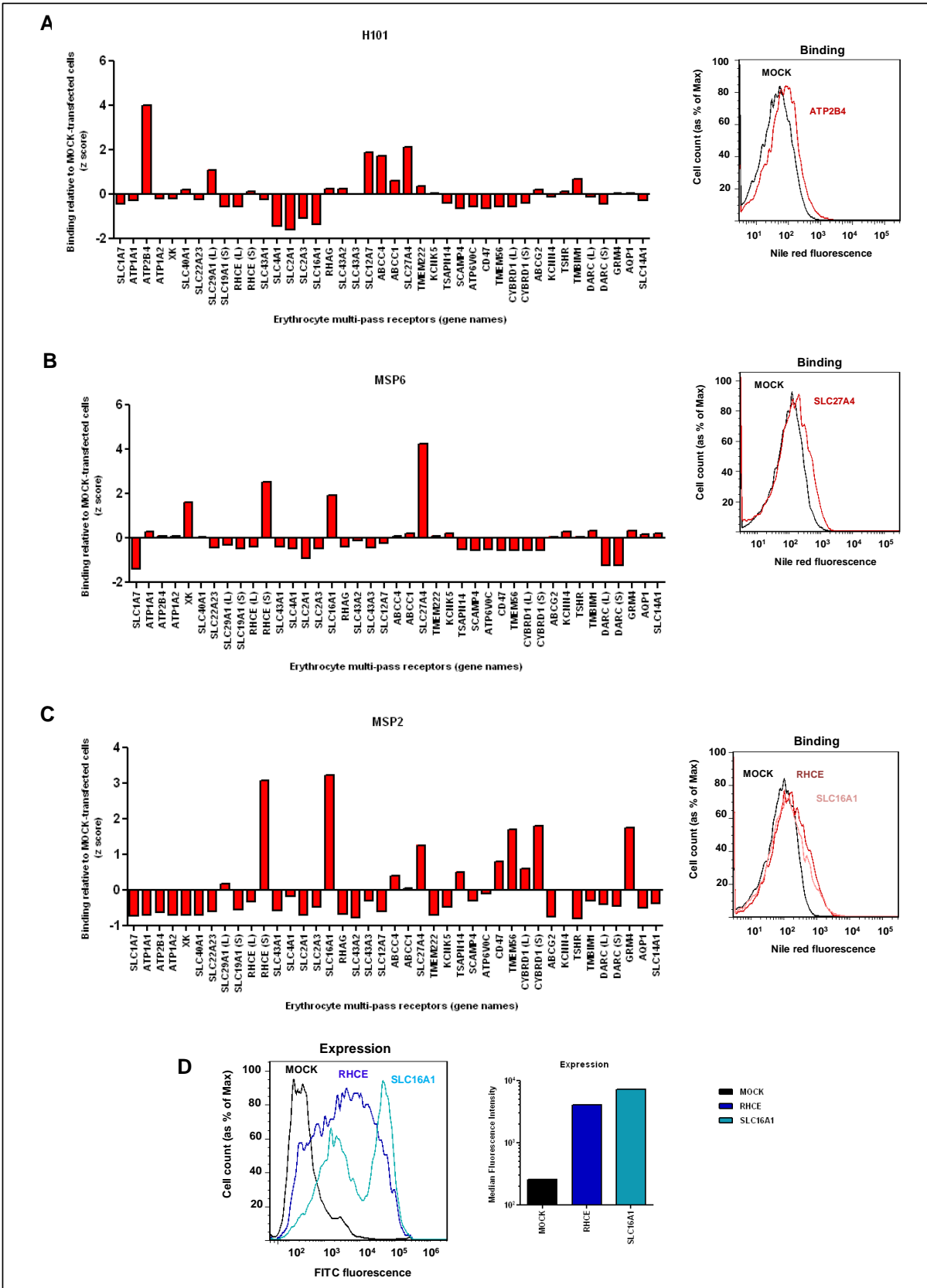


Figure 56. The *P. falciparum* proteins H101, MSP6 and MSP2 showed significant binding (z scores above 3) to specific recombinant multi-pass receptors. A), B) and C) The bar charts show the normalised binding (z scores) of H101 (A), MSP6 (B) and MSP2 (C) to the panel of erythrocyte multi-pass receptors. The histograms represent mock-transfected cells (black) and cells transfected with ATP2B4 (red) (A), SLC27A4 (red) (B), RHCE (red) (C) and SLC16A1 (pink) (C), after incubation with AARP-coated Nile red beads. **D)** The histograms are of mock-transfected cells (black) and cells transfected with RHCE (dark blue) or SLC16A1 (light blue), stained with an anti-c-Myc mouse monoclonal and a FITC-conjugated anti-mouse secondary. The bar chart shows the median fluorescence intensities (at the FITC emission wavelength) of the antibody stained cells. ATP2B4, SLC27A4, RHCE and SLC16A1, code for the multi-pass receptors Plasma membrane calcium transporting ATPase 4, Fatty acid transporter 4, Rh blood CE group antigen polypeptide and Monocarboxylate transporter 1, respectively.

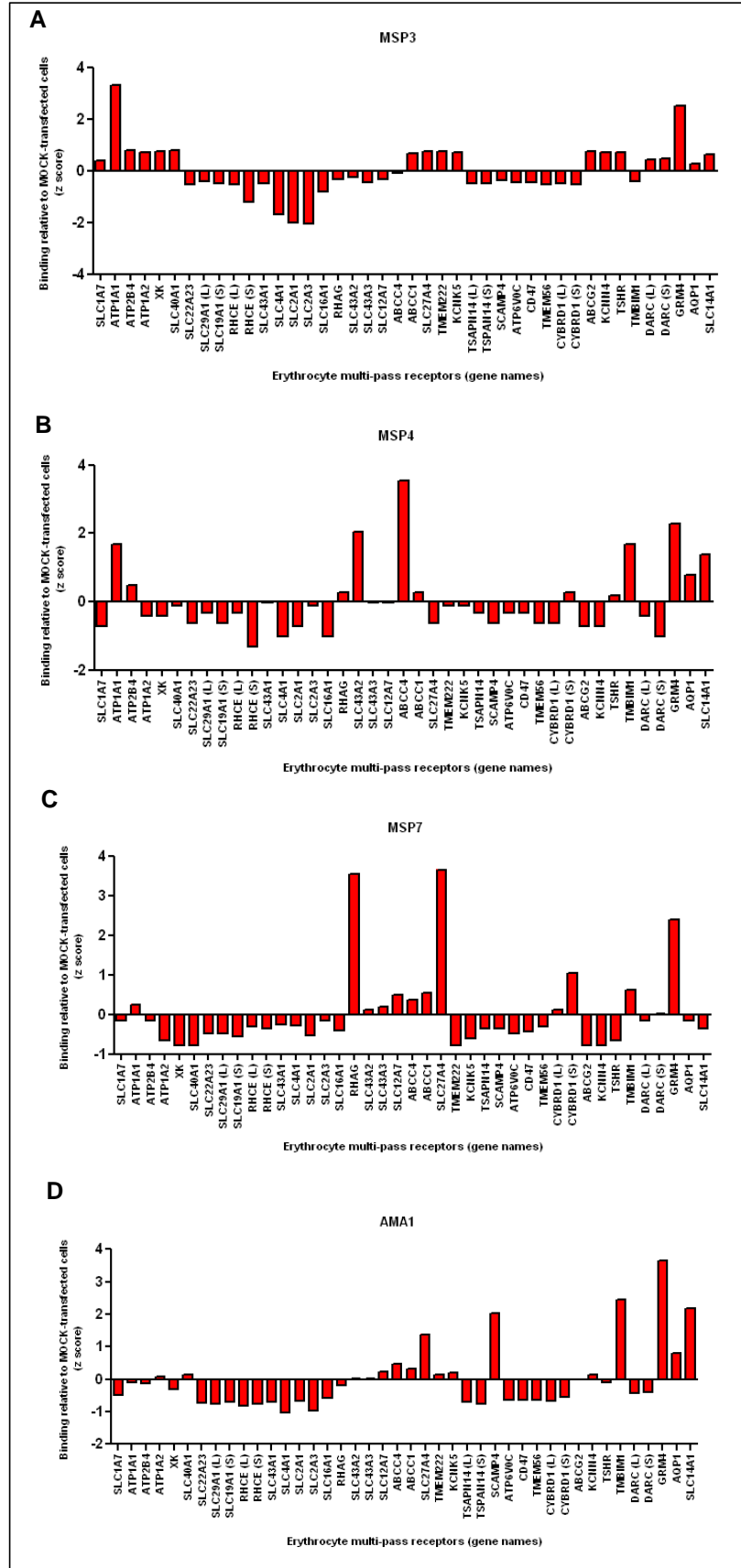


Figure 57. Significant (z scores above 3) binding to specific recombinant multi-pass receptors was also observed with the *P. falciparum* proteins MSP3, MSP4, MSP7 and AMA1. A), B), C) and D) The bar charts show the normalised binding (z scores) of MSP3 (A), MSP4 (B), MSP7 (C) and AMA1 (D) to the panel of erythrocyte multi-pass receptors.

blood group associated protein (RHAG) and Metabotropic glutamate receptor 4 (GRM4) respectively, also had relatively significant z scores of above 3 (Figure 57). No binding of the MSP1 protein to Band 3 was seen in the screen (Figure 58 A and B). Compared to mock-transfected cells, cells expressing Band 3 showed higher binding only to RH5 (Figure 58 C). The z score of this interaction was however less than 2, indicating that it wasn't very significant and probably a result of a slight up-regulation in the expression of Basigin (Figure 58 D).

5.2.7 Preliminary follow-up study: recapitulation of the interaction between AARP and the Fatty acid transporter 4.

The attempt to recapitulate the interaction between AARP and the Fatty acid transporter 4, using an independent preparation of AARP and a fresh batch of cells transfected with its putative erythrocytic receptor was successful (Figure 59). The level of expression of the recombinant receptor was less than what was observed in the original screen (Figure 59 A) and perhaps as a consequence the difference in the binding of AARP to mock-transfected cells and to those transfected with the Fatty acid transporter 4 was also lower (Figure 59 B).

5.2.8 Investigating the carbohydrate-binding properties of nine proteins selected from the *P. falciparum* merozoite surface protein library.

When tested against untreated HEK293E cells in a previous screen, 15 of the *P. falciparum* merozoite surface proteins showed some putative binding. It is likely that at least some of these proteins were recognising specific carbohydrate moieties at the cell surface and indeed the binding of four of the proteins, namely Pf113, EBA140, EBA175 and MSRP2, was observed to be dependent on sialic acid (Figure 51). To probe their glycan-binding properties further, these four proteins and five others (Pf12, RhopH3, AARP, MSP3.4 and MSP3.8) which had shown

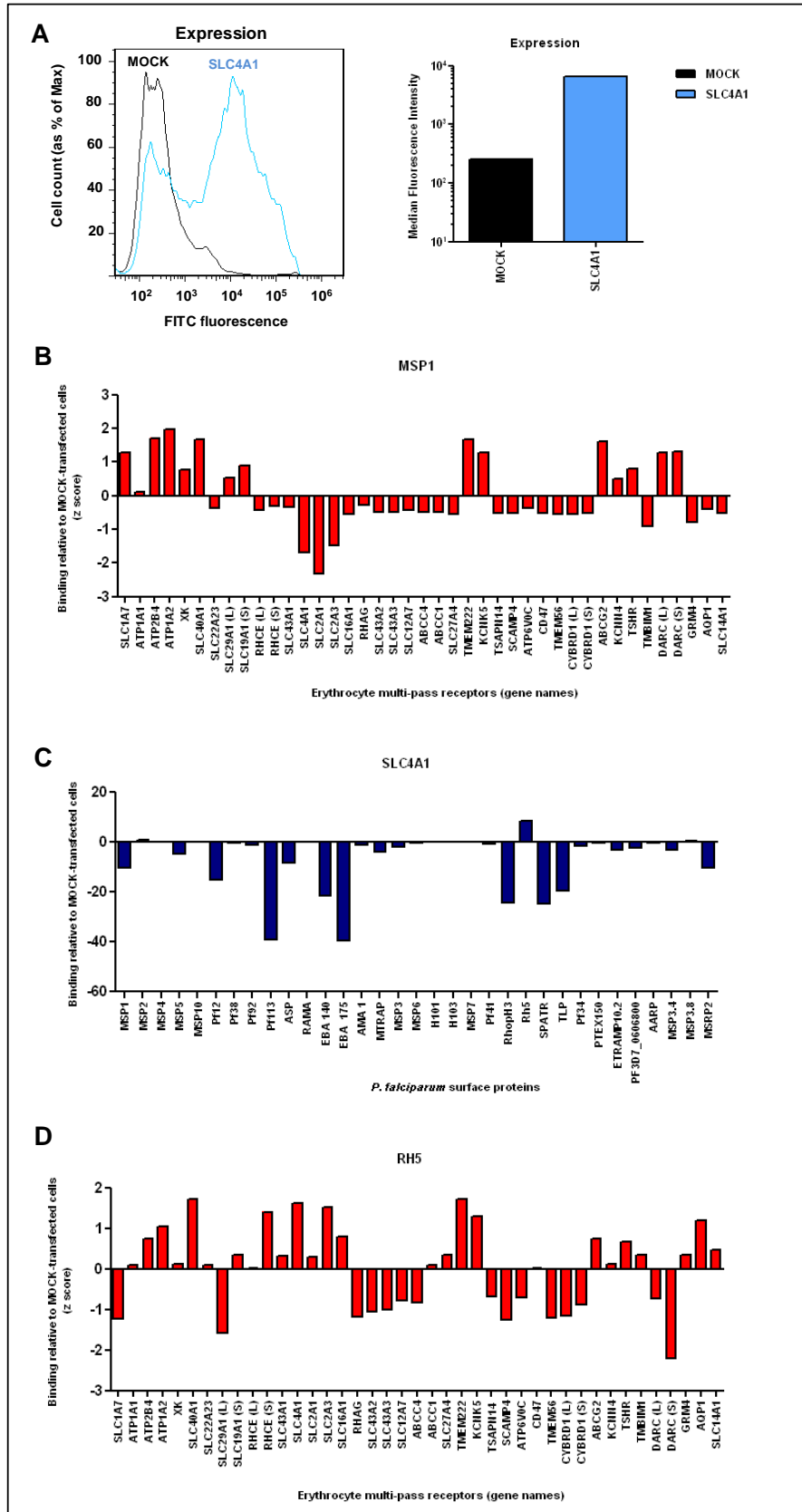


Figure 58. No binding between the *P. falciparum* protein MSP1 and the erythrocyte multi-pass receptor Band3 (gene name: SLC4A1) was detected in the screen. **A)** The histograms are of mock-transfected cells (black) and cells transfected with SLC4A1(blue), stained with an anti-c-Myc mouse monoclonal and a FITC-conjugated anti-mouse secondary. The bar chart shows the median fluorescence intensities (at the FITC emission wavelength) of the antibody stained cells. **B)** and **D)** The bar charts represent the normalised binding (z scores) of MSP1 (**B**) and Rh5 (**D**) to the panel of erythrocyte multi-pass receptors. **C)** The non-normalised binding of the library of *P. falciparum* proteins to SLC4A1-transfected cells, relative to mock-transfected cells is shown.

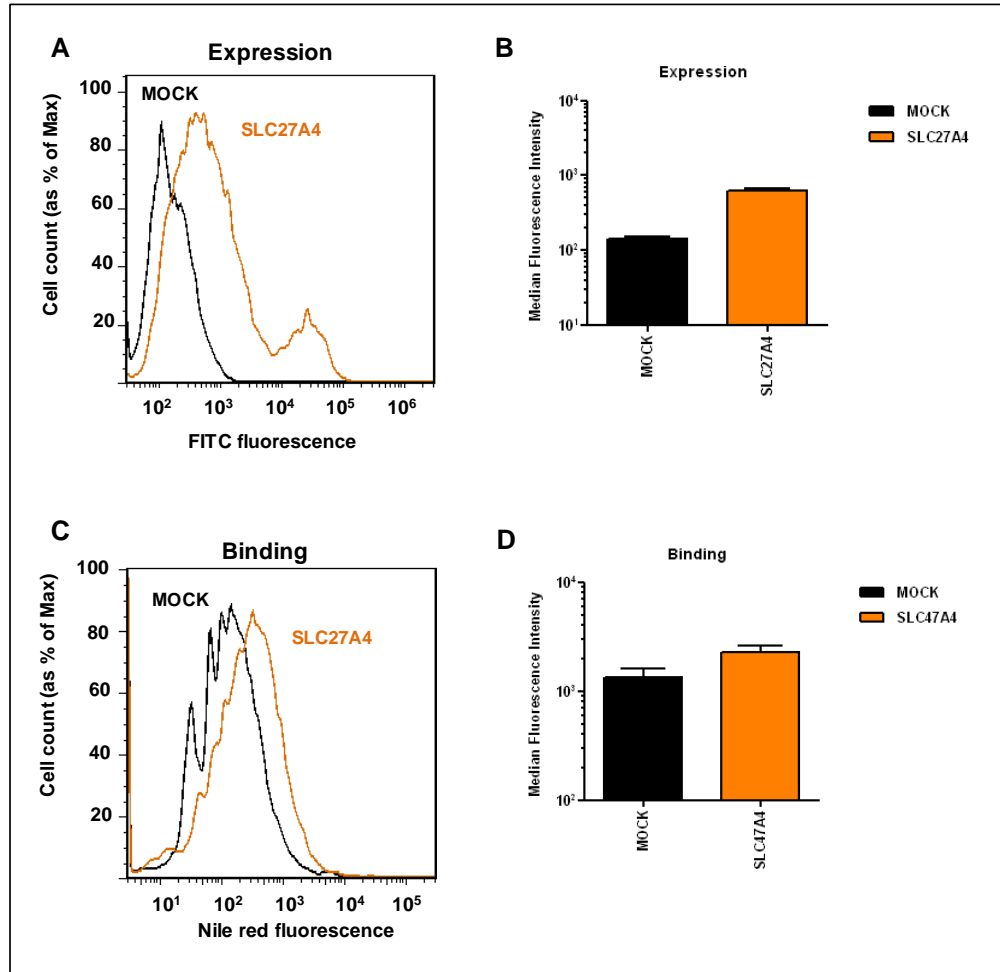


Figure 59. The interaction between the *P. falciparum* protein AARP and the recombinant multi-pass receptor, Fatty acid transporter 4 (gene name: SLC27A4) was recapitulated in an independent follow-up experiment, using the same assay as in the original screen. **A)** and **B)** The histograms are of mock-transfected cells (black) and cells transfected with SLC27A4 (yellow), stained with an anti-c-Myc mouse monoclonal and a FITC-conjugated anti-mouse secondary. The bar chart shows the median fluorescence intensities (at the FITC emission wavelength) of the antibody stained cells. **C)** and **D)** The histograms show mock-transfected cells (black) and cells transfected with SLC27A4 (yellow) (**A**), after incubation with AARP-coated Nile red beads. The bar chart shows the median fluorescence intensities (at the Nile red emission wavelength) of the cells.

sialic-acid independent binding to HEK293E cells, were selected for testing against a panel of synthetic glycan probes in a pilot screen. The synthetic glycan probes used were purchased commercially from GlycoTech and included antigens of the ABH, Lewis, P₁, T, Tn blood types as well individual monosaccharides and the core glycan components of N-linked and O-linked oligosaccharides (Table 8 and Figure 60 A). In the screen, biotinylated forms of the glycans were immobilised on a streptavidin-coated plate and probed with the *P. falciparum* surface proteins expressed as β lactamase-tagged, pentameric preys. Binding events were detected using the β -lactamase substrate nitrocefin.

Prior to performing the screen, the well-characterised interaction between the human protein P-selectin and its carbohydrate ligand sialyl-Lewis X (sialyl-Le^x) was used in a proof-of-principle study to assess the technical feasibility and specificity of the assay (Polley *et al.*, 1991). P-selectin, also expressed as a β -lactamase-tagged pentamer was observed to bind to the synthetic sialyl- Le^x probe and this Ca²⁺-dependent interaction could be inhibited by the addition of EDTA in a concentration-dependent manner (Figure 60 C).

In the screen, any significant binding to the carbohydrate probes was seen only with Pf113, EBA140, EBA175 and MSRP2 (Figures 61, 62 and 63). These four proteins, which showed sialic-acid dependent binding to HEK293E cells, also recognised carbohydrate probes containing sialic-acid (Figures 62 and 63). The binding of each of these proteins to a number of sialic acid-containing but structurally different glycans needs to be investigated.

Table 8. The panel of 55 synthetic carbohydrate probes.

Number	Glycan	Structure
1	α -D-Glucose	Monosaccharide
2	β -D-Glucose	
3	α -D-Galactose	
4	β -D-Galactose	
5	α -D-Mannose	
6	α -D-Man-6-phosphate	
7	α -L-Fucose	
8	β -GlcNAc	
9	α -GalNAc (T _n antigen)	
10	β -GalNAc	
11	α -Neu5Ac	
12	GalNAc α 1-3Gal β (A antigen)	Disaccharide
13	Gal α 1-3Gal β (B antigen)	
14	Fuc α 1-2Gal β (H antigen)	
15	Gal β 1-3GlcNAc β (Le ^c antigen)	
16	Gal β 1-4Glc β (Lactose)	
17	Gal β 1-4GlcNAc β (N-acetyllactosamine, LacNAc)	
18	Gal β 1-3GalNAc α (O-glycan core 1)	
19	Fuc α 1-3GlcNAc β (Le antigen)	
20	Fuc α 1-4GlcNAc β (Le antigen)	
21	GalNAc α 1-3GalNAc β	
22	Gal α 1-3GalNAc α (T _{aa} antigen)	
23	Gal β 1-3GalNAc β (T _{bb} antigen)	
24	Gal α 1-3GalNAc β (T _{ab} antigen)	
25	Gal β 1-3Gal β	
26	GalNAc α 1-3(Fuc α 1-2)Gal β (A antigen)	Trisaccharide
27	Gal α 1-3(Fuc α 1-2)Gal β (B antigen)	
28	Le ^a antigen	
29	Le ^x antigen	
30	3'-Sialyllactose	
31	6'-Sialyllactose	
32	Le ^b antigen	Complex oligosaccharide
33	Le ^y antigen	
34	Sialyl Le ^a	
35	Sialyl Le ^x	Monosaccharide
36	Neu5Gca	Disaccharide
37	GlcNAc β 1-3Gal β	
38	Gal α 1-4GlcNAc β (α -N-acetyllactosamine)	
39	Glc α 1-4Glc β (Maltose)	
40	Gal β 1-3GalNAc α (TF antigen)	
41	Neu5Ac α 2-6GalNAc α (6-SiaT _n)	
42	H antigen (type 3)	
43	Neu5Ac α 2-3Gal (Sialylated galactose)	
44	GlcNAc β 1-3GalNAc α (N-glycan core 3)	
45	GlcNAc β 1-6GalNAc α (N-glycan core 6)	
46	Neu5Ac α 2-3Gal β 1-4GlcNAc β (Sialyl-LacNAc)	Trisaccharide
47	Neu5Ac α 2-8Neu5Ac α 2-8Neu5Ac α (Polysialic acid)	
48	Gal β 1-3(GlcNAc β 1-6)GalNAc α (O-glycan core 2)	
49	Neu5Ac α 2-3Gal β 1-3GalNAc α (O-glycan Sia-core1)	
50	GlcNAc β 1-3(GlcNAc β 1-6)GalNAc α	Complex
51	Gal β 1-3GlcNAc β 1-3Gal β 1-4Glc β (LNT)	
52	Gal β 1-4GlcNAc β 1-3Gal β 1-4Glc β (LNnT)	
53	Neu5Gca2-6GalNAc α	Monosaccharide
54	Neu5Ac α 2-3GalNAc α (3-SiaT _n)	Trisaccharide
55	Gal α 1-4Gal β 1-4GlcNAc β (P ₁ antigen)	

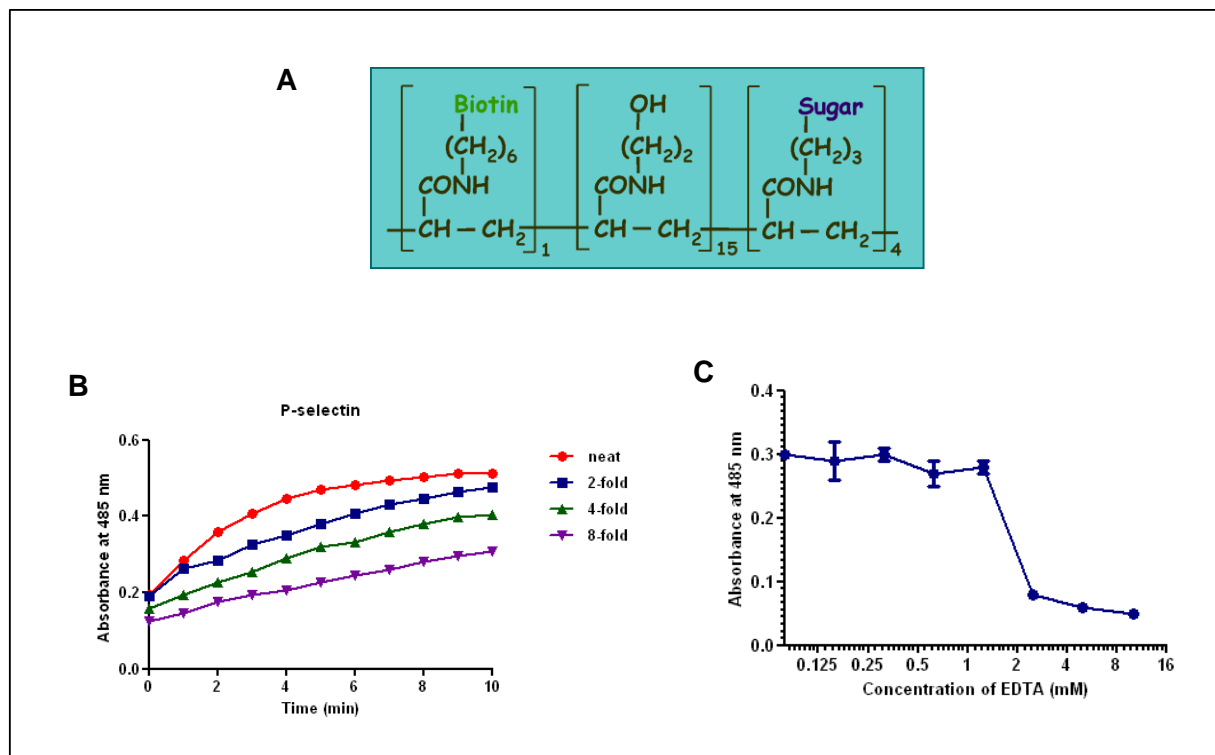


Figure 60. A ‘proof-of-principle’ study: the human protein P-selectin showed specific binding to synthetic sialyl-Le^x. P-selectin, expressed as a β -lactamase tagged pentamer (with C-terminal Cd4), was probed against biotinylated sialyl- Le^x immobilised on a streptavidin-coated plate. After incubation for 2 h at room temperature, putative protein-glycan binding was detected by the turnover of the β -lactamase substrate, nitrocefin at an absorbance of 485 nm. **A)** The synthetic sialyl-Le^x probe used was attached to a biotin tag via a flexible linker. The schematic was reproduced from the GlycoTech webpage <http://www.glycotech.com/probes/multivalbio.html>. **B)** The level of expression of the P-selectin protein was estimated by monitoring the turnover of nitrocefin in a time course assay. A 2-fold dilution series of the protein was used for this purpose. The protein was used neat for testing against the glycan probe. **C)** The graph shows the Ca²⁺-dependent binding of P-selectin to synthetic sialyl- Le^x. The assay was performed in the presence of a range of different concentrations of EDTA, from 0.08- 10 mM. The data is shown as mean \pm standard deviation, n=3.

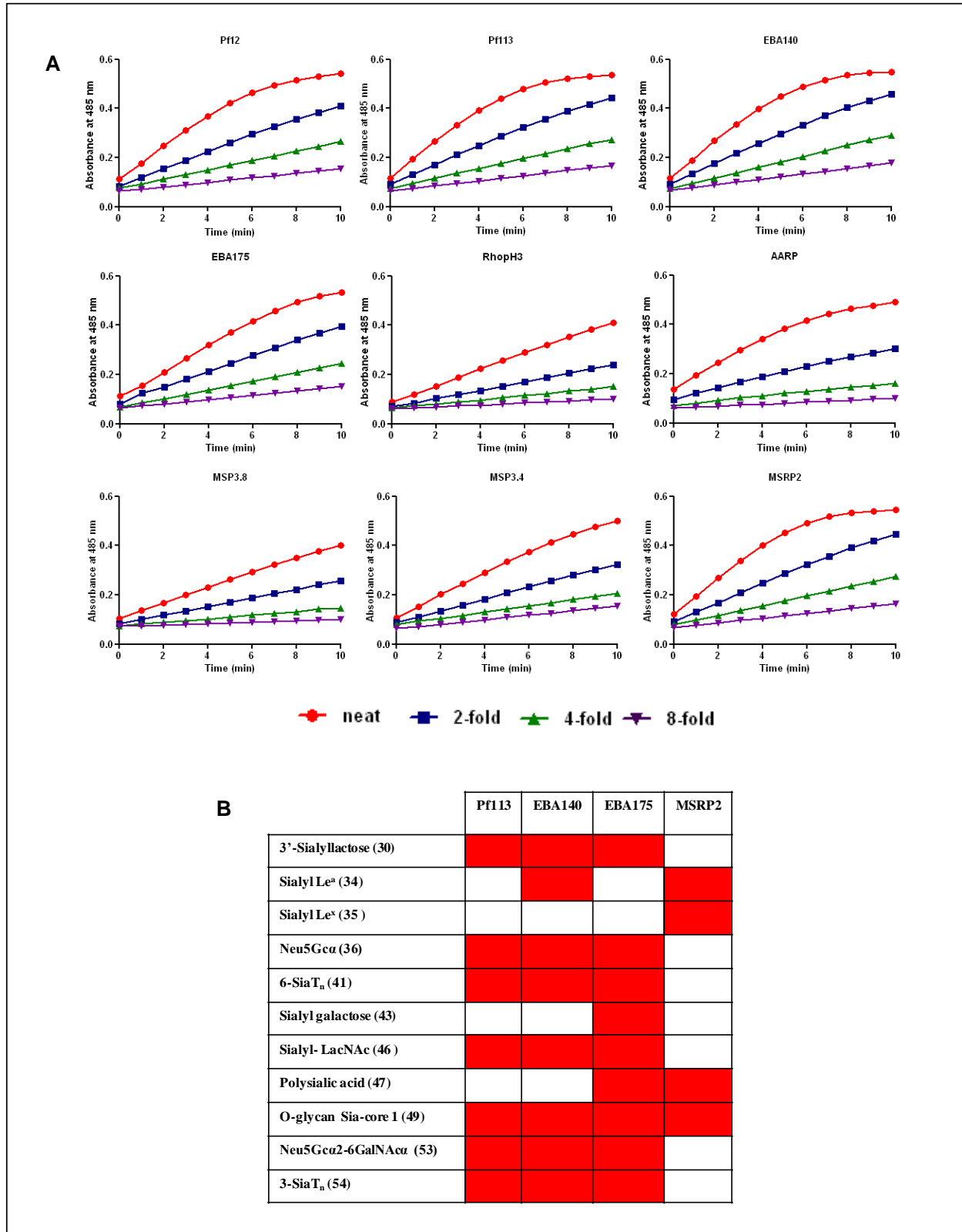


Figure 61. Nine *P. falciparum* proteins were screened against a panel of 55 synthetic glycan probes. The *P. falciparum* proteins expressed as β lactamase-tagged pentamers (with C-terminal Cd4) were tested against the biotinylated glycans immobilised on streptavidin-coated plates. Protein-glycan binding was detected by the turnover of nitrocefin at 485 nm. **A)** The *Plasmodium* proteins were normalised against each other, by monitoring the turnover of nitrocefin in a time course assay. **B)** In the screen, four of the proteins showed binding to glycans containing sialic acid. Red indicates an interaction.

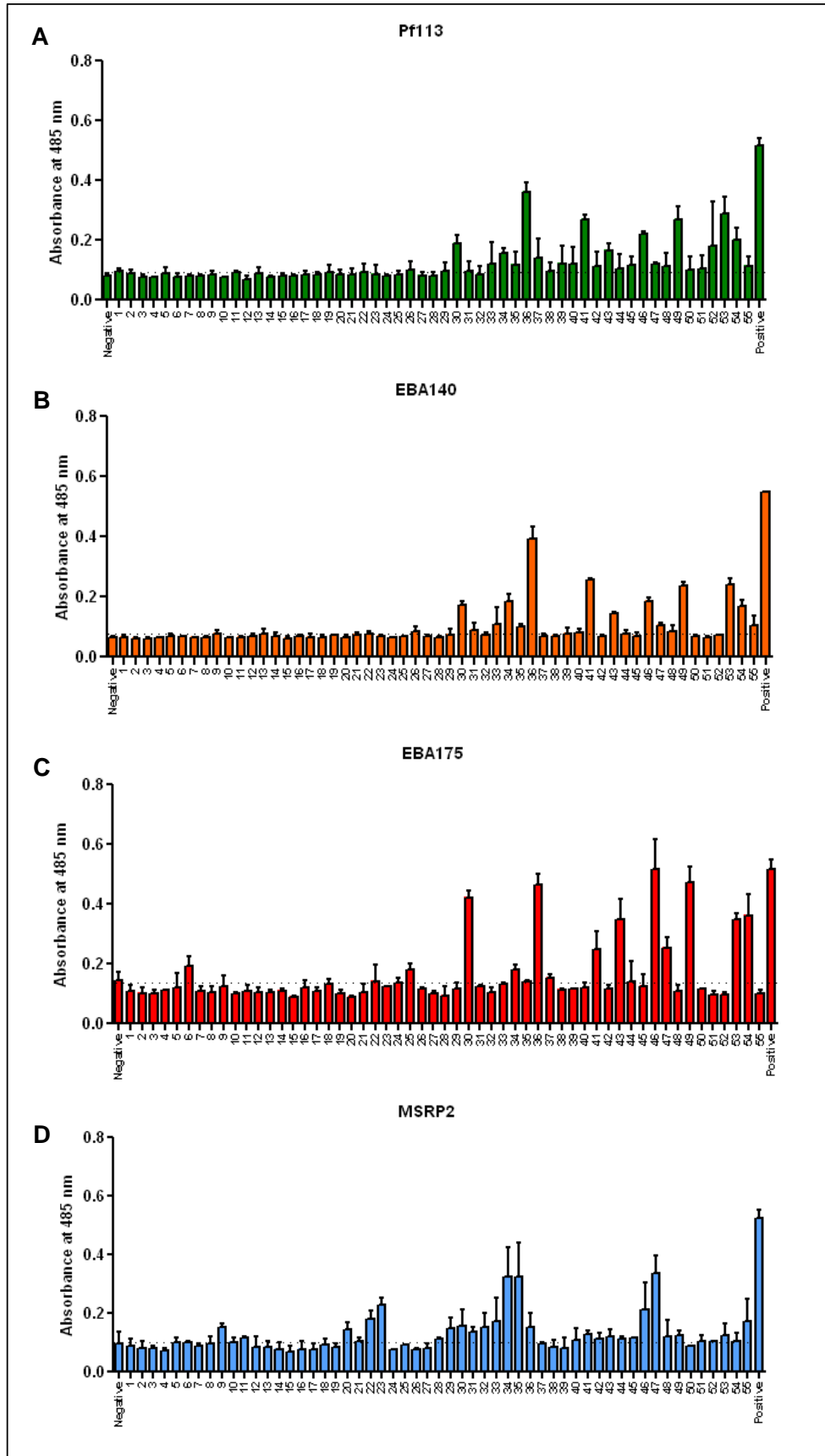


Figure 62. Four *P. falciparum* proteins tested showed binding to sialic acid-containing glycans. The bar charts show the binding of Pf113, EBA140, EBA175 and MSRP2 to the panel of 55 synthetic glycan probes. Each bar shows mean \pm standard deviation, n=2. Biotinylated OX68 (an anti-Cd4 monoclonal) was used as the positive control bait in the screen. The biotinylated bait used as the negative control contained the linker region carried by all the synthetic glycans.

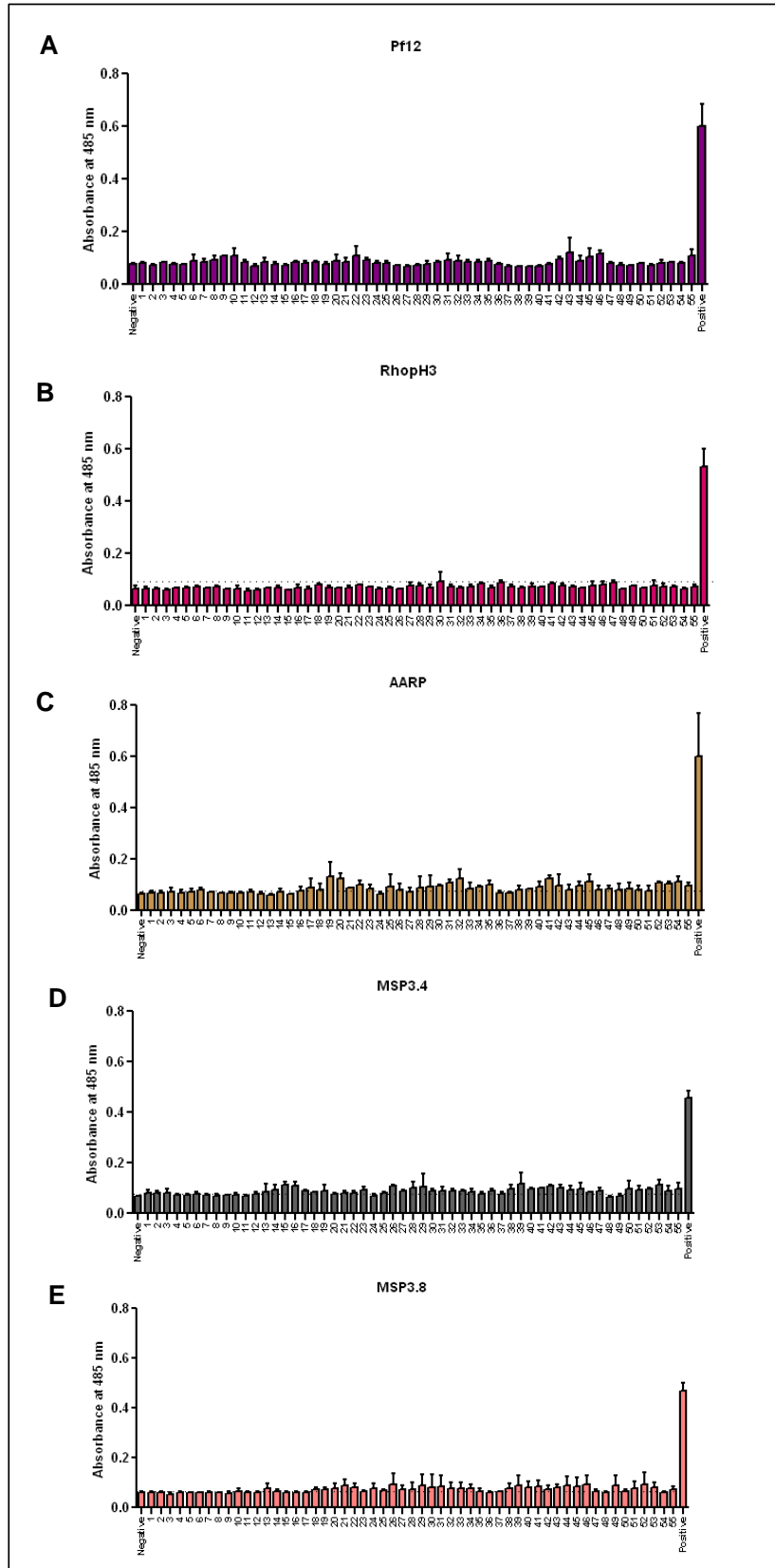


Figure 63. Five *P. falciparum* proteins tested showed no significant binding to any glycan. The bar charts show the binding of Pf12, RhopH3, AARP, MSP3.4 and MSP3.8 to the panel of 55 synthetic glycan probes. Each bar shows mean \pm standard deviation, n=2. Biotinylated OX68 (an anti-Cd4 monoclonal) was used as the positive control bait in the screen. The biotinylated bait used as the negative control contained the linker region carried by all the synthetic glycans.

5.3 DISCUSSION

An efficacious vaccine against malaria is vital for sustained control and eradication of this disease on a worldwide scale (Crompton *et al.*, 2010). As the causative agent of the most clinically severe form of malaria, *P. falciparum* has been the primary focus of attempts to develop such a vaccine over the past three decades. Candidate vaccines that target only one particular stage of the *P. falciparum* life cycle have been observed to be incapable of conferring complete sterile protection against malaria, in clinical trials (Geels *et al.*, 2011; Greenwood and Targett, 2011). A potentially more successful approach is to combine several antigens from different stages of the parasite life cycle in a multi-component vaccine. *P. falciparum* merozoite surface proteins that play an important role in erythrocyte invasion are ideal candidates for the blood stage component of such a next-generation vaccine (Tham *et al.*, 2012). Transcriptomic and proteomic studies have identified around 260 proteins that are expressed at the merozoite stage in *P. falciparum*, however, more than 70% of these have no identified function (Bozdech *et al.*, 2003; Florens *et al.*, 2002). In order to determine which of the novel *P. falciparum* merozoite surface proteins should be prioritised as potential vaccine candidates, their functional characterisation with the use of large-scale, high-throughput techniques is therefore, a necessity (Tran *et al.*, 2005).

Traditional methods used for identifying protein-protein interactions on a global scale, such as yeast-2-hybrid screening and tandem affinity purification-mass spectrometry cannot be used for detecting the low-affinity extracellular interactions between *P. falciparum* merozoite surface proteins and erythrocyte receptors (Bei and Duraisingh, 2012; Wright, 2009). Similarly the commonly used methods for identifying the binding of *P. falciparum* surface proteins to

erythrocytes (e.g. erythrocyte ‘rosetting’ assays) are not amenable for adaptation to high-throughput screening (Tran *et al.*, 2005).

The AVEXIS platform developed in our laboratory is designed to facilitate the detection of low-affinity interactions between proteins in a high-throughput manner and has been used successfully to identify novel interactions between a library of *P. falciparum* merozoite surface proteins and a panel of erythrocyte receptors, expressed as full-length ectodomain fragments (Crosnier *et al.*, 2011; Bartholdson *et al.*, unpublished data). The expression of proteins in soluble form is however a pre-requisite of this ELISA-based screening strategy and it is thus not applicable to multi-pass receptors.

In this study, a novel flow cytometry-based approach was used to screen the library of *P. falciparum* surface protein ectodomains against both human erythrocytes and recombinant erythrocyte multi-pass receptors expressed on HEK293E cells, in a high-throughput manner. An ELISA-based assay was also developed for identifying the glycan-binding properties of *P. falciparum* surface proteins, by screening against a panel of synthetic carbohydrate probes.

5.3.1 Investigating the binding of a library of *P. falciparum* merozoite surface proteins to human erythrocytes using a novel high-throughput, flow cytometry-based approach.

From the 33 *P. falciparum* proteins which were presented to human erythrocytes as multimeric arrays on Nile red beads, 13 showed some association with the erythrocyte surface (Figure 45). Of these, the interactions of EBA175, EBA140, RH5, Pf34, MSP3.4 and MSP3.8 were the most significant. In this assay, the binding of a bead-immobilised parasite protein to a receptor on the erythrocyte surface, was expected to cause an increase in the fluorescence intensity of the erythrocyte population (at the Nile red emission wavelength). The magnitude of this ‘shift’ in fluorescence would be proportional to the number of protein-coated beads associated with each

erythrocyte, which in turn would be dependent on the copy number/cell of the erythrocyte receptor recognised by the parasite protein. The largest shifts in the fluorescence intensity of the erythrocyte populations (i.e. the highest levels of binding) were seen with EBA175 and EBA140, the two parasite proteins known to recognise the highly abundant receptors, Glycophorins A and C, respectively (Figure 45). The other 11 parasite proteins, including RH5, seemed to interact with erythrocyte receptors which were present at much lower abundance. Probing the specificity of the observed interactions by enzymatic pre-treatment of erythrocytes revealed that EBA140 binds to erythrocytes in a trypsin and neuraminidase sensitive but chymotrypsin insensitive manner, which is consistent with its known sialic acid dependent binding to Glycophorin C (Figures 46). On the other hand, the binding of RH5 to erythrocytes was insensitive to treatment with trypsin, chymotrypsin and neuraminidase, which is in agreement with the enzymatic susceptibility profile of the interaction between RH5 and its known erythrocyte receptor, Basigin (Figure 46). The binding of the proteins, Pf34, MSP3.4 and MSP3.8, to erythrocytes was also not affected by treatment with any of the three enzymes (data not shown). These proteins may be interacting with multi-pass receptors, which are less susceptible to proteolytic digestion or with non-proteinaceous receptors such as glycolipids. Pf34 is a GPI-anchored protein, located in detergent-resistant membrane domains in the rhoptry neck of the parasite and synthetic peptides based on its sequence have been shown to inhibit erythrocyte invasion by *P. falciparum*, albeit at relatively high concentrations (Proellocks *et al.*, 2007; Arévalo-Pinzón *et al.*, 2010). MSP3.4 and MSP3.8, peripheral surface proteins of the MSP3-multigene family, are targets of naturally-acquired protective antibodies against *P. falciparum* infection (Singh *et al.*, 2009). Pf34, MSP3.4 and MSP3.8 are therefore likely to be involved in interactions with erythrocyte surface receptors.

In comparison to traditional erythrocyte binding assays, the flow-cytometry based assay used in this study is fast, simple, quantitative and objective. It also incurs very little sample consumption. Immobilisation of parasite ligands on fluorescent beads was performed using small volumes (~100 µl per reaction on average) of cell culture supernatants containing the recombinantly-expressed proteins, with no prior purification. The biggest strength of this assay however is its amenability to high throughput screening, as demonstrated by testing with 33 *P. falciparum* surface proteins in parallel. Interactions with erythrocyte receptors of very low abundance are however likely to be missed with this approach, which is a major drawback. Based on the observations to date, this assay is probably most suitable for use in preliminary screens to narrow down large libraries of *Plasmodium* proteins to smaller selections of putative erythrocyte-binding ligands, which can then be characterised further using the traditional binding assays.

5.3.2 Screening *P. falciparum* merozoite surface proteins against a panel of erythrocyte multi-pass receptors expressed recombinantly on HEK293E cells, to identify novel interactions.

The major focus of the work described in this chapter, was the screening of the *P. falciparum* surface protein library against a panel of erythrocyte multi-pass receptors to identify novel interactions. The 41 erythrocyte receptors selected were expressed individually on the surface of HEK293E cells, in recombinant form, for this purpose and probed with multimeric bead-based arrays of the parasite proteins.

5.3.2.1 Endogenous receptors on HEK293E cells were recognised by some *P. falciparum* proteins.

Of the 33 *P. falciparum* proteins tested in the screen, 15 showed some ‘background’ binding to untreated and mock-transfected HEK293E cells, the expression host of the recombinant

erythrocyte multi-pass receptors (Figure 50). The highest binding was observed with the proteins RH5, EBA140, MSP3.4, MSP3.8, Pf12, MSRP2 and Pf113. Of these, some binding to human erythrocytes was previously observed with RH5, EBA140, MSP3.4, MSP3.8, Pf12 and MSRP2, suggesting that they are potentially binding to receptors present on both erythrocytes and HEK293E cells. Indeed, staining HEK293E cells with specific monoclonals revealed high endogenous expression of Basigin, accounting for the binding of RH5 to these cells (Figure 52).

Pf12 is a GPI-anchored protein located in detergent-resistant membrane domains at the merozoite surface (Sanders *et al.*, 2005). It has been implicated in erythrocyte attachment, due to the presence of dual six-cysteine domains, a fold that is also found in some adhesive proteins expressed at other life cycle stages of the parasite (Carter *et al.*, 1995; Sanders *et al.*, 2005). MSRP2 is a member of the MSP7-multigene family, expressed at the asexual erythrocytic stage of the parasite. It has been identified as a potential substrate of the SUB1 protease which also cleaves MSP7 and MSP1 amongst others (Kadekoppala *et al.*, 2010; Silmon de Monerri *et al.*, 2011). Deletion of MSRP2 has however been found to have no effect on erythrocyte invasion and growth of *P. falciparum*, suggesting that it's likely to be functionally redundant (Kadekoppala *et al.*, 2010).

Pf113 showed clear binding to HEK293E cells but not to erythrocytes (Figures 45 and 50), suggesting that it may be interacting with a surface receptor which is either absent on human erythrocytes or present only at very low levels. Pf113 is a putative GPI-anchored protein with cysteine-rich domains, located in lipid rafts and expressed both in the sporozoites and the merozoite stages of the *P. falciparum* life cycle (Sanders *et al.*, 2005; Obando-Martinez *et al.*, 2010).

Pre-treatment of HEK293E cells with neuraminidase significantly reduced the binding of EBA140, Pf113 and MSRP2 suggesting sialic-acid dependent recognition of surface receptors (Figure 51).

5.3.2.2 A number of potential erythrocyte multi-pass receptor: *P. falciparum* ligand pairs were identified in the screen.

A total of 13 putative interactions between erythrocyte multi-pass receptors and *P. falciparum* surface proteins were identified in the screen (Figures 54-57). The two most significant interactions were those between the *P. falciparum* protein AARP and the erythrocyte receptor Fatty acid transporter 4 (gene name: SLC27A4) and between the parasite protein MSP11 and the erythrocytic Plasma membrane calcium transporting ATPase 4 (ATP2B4) (Figure 55). AARP is a rhoptry protein, antibodies against which have been detected in malaria-immune individuals (Wickramarachchi *et al.*, 2008). There is also some evidence to indicate binding of this protein to human erythrocytes (Wickramarachchi *et al.*, 2008). MSP11, a member of the MSP3 family, is a peripheral protein associated with the merozoite surface (Pearce *et al.*, 2005). Transfected parasite lines expressing truncated forms of MSP11 are viable, which suggests that this protein is not essential for blood-stage growth (Pearce *et al.*, 2005).

Fatty acid transporter 4, belongs to a family of multi-pass receptors responsible for the cellular uptake and activation of long-chain fatty acids. This ~71 kDa protein is expressed in a relatively broad range of tissues (e.g. heart, liver, pancreas, adipose tissue) and mutations in its gene, SLC27A4, have so far been associated with the Ichthyosis prematurity (a keratinisation disorder which causes epidermal abnormalities) and insulin resistance syndromes, but not malaria (Gertow *et al.*, 2004; Klar *et al.*, 2009). On the other hand, single nucleotide polymorphisms in ATP2B4, the gene coding for the Plasma membrane calcium transporting ATPase 4, have been

found to correlate strongly with resistance against severe *P. falciparum* malaria in a West African population (Timmann *et al.*, 2012). The intra-erythrocytic growth of *P. falciparum* is dependent on the presence of high levels of Ca^{2+} (Deasi *et al.*, 1996). Therefore, mutations in ATP2B4 have been proposed to directly influence parasite growth by causing changes to the level of expression or structure of the erythrocytic Ca^{2+} pump (Timmann *et al.*, 2012). However, the possibility of these mutations conferring protection against *P. falciparum* infection by preventing an interaction between the Ca^{2+} pump and a parasite ligand, which is important for erythrocyte invasion, cannot be excluded.

5.3.2.3 Further validation/characterisation of putative interactions between parasite proteins and recombinant multi-pass receptors.

On the surface of transiently-transfected HEK293E cells, the recombinant multi-pass receptors are displayed amongst a multitude of other surface proteins, lipids and glycans, any of which may be a target of particular *P. falciparum* merozoite proteins. In this screen, the binding of *P. falciparum* proteins to mock-transfected cells was subtracted from the binding to cells transiently-expressing each recombinant multi-pass receptor, in order to remove any such ‘background’ binding to endogenous HEK293E cell components. However, up- or down-regulation of particular endogenous surface receptors, as a direct or indirect consequence of the expression of exogenous DNA, could have led to confounding results in the binding assays. The up-regulation of unrelated endogenous receptors in particular could have resulted in the identification of ‘false positives’ in the screen.

When validating the potential interactions identified in the screen, the recombinant multi-pass receptors should ideally be incorporated into synthetic lipid bilayers, in order to eliminate any ‘false positives’ which resulted from the binding of the parasite proteins to endogenous

HEK293E cell components. The compositions of artificial membrane mimetics can be closely regulated, unlike those of native membranes. Erythrocytic multi-pass receptors reconstituted in such artificial bilayers can be tested for direct interaction with their putative parasite ligands using SPR, Backscattering Interferometry (BSI) or Isothermal Titration Calorimetry (ITC), all of which have been used with some success, to investigate the biomolecular interactions of integral membrane proteins, incorporated in to synthetic lipid bilayers (Baksh *et al.*, 2011; Maynard *et al.*, 2010; Sikora & Turner, 2005). These techniques allow the affinities of the interactions to be quantified, which is an advantage over flow-cytometry based approaches.

It is also necessary to investigate the importance of the identified receptor-ligand interactions for invasion of human erythrocytes by *P. falciparum*. For this purpose, antibodies raised against the multi-pass receptors should first be selected for blocking of the interaction with the parasite ligand *in vitro* and then tested for inhibition of erythrocyte entry by *P. falciparum* in functional assays (Crosnier *et al.*, 2011).

5.3.3 The glycan-binding properties of a selected subset of merozoite surface proteins were tested by screening against a panel of synthetic carbohydrate probes.

In this study, a high-throughput ELISA-based method was used to identify the glycan-binding properties of a number of selected *P. falciparum* proteins. Each parasite protein, expressed as a soluble enzyme-tagged pentamer was tested against a panel of 55 synthetic biotinylated carbohydrate probes, immobilised on streptavidin-coated plates. The panel of glycans screened included a number of blood group antigens (Table 8). Five of the *P. falciparum* proteins tested, including Pf12, AARP, MSP3.4 and MSP3.8 showed no binding to any of the glycans (Figure 63). Recognition of sialic-acid containing glycans was observed with EBA175, EBA140, Pf113 and MSRP2, all of which had been observed to interact with erythrocytes and/or HEK293E cells

in a neuraminidase-sensitive manner (Figure 62). The binding of each of these latter four proteins to a number of sialic acid-containing but structurally-different glycans requires further investigation. Analysis of these protein-glycan interactions by SPR, for example, can reveal potential differences in the affinity of the parasite ligands for the variant glycan structures, indicating which is preferred. Glycans are also covalently-linked to proteins or lipids on the erythrocyte membrane, therefore specificity may come from the dual recognition of both the glycan and the protein/lipid backbone by the *P. falciparum* proteins.

5.4 CONCLUSION

In this study, new high-throughput screening strategies were developed for investigating the binding of *P. falciparum* merozoite surface proteins to human erythrocytes, recombinantly-expressed erythrocytic multi-pass receptors and glycans. A number of novel interactions were identified by the performed screens and are now awaiting further characterisation; including the binding of Pf34, MSP3.4 and MSP3.8 to human erythrocytes, the recognition of the multi-pass receptor Fatty acid transporter 4 by AARP and the binding of sialic acid by Pf113. Such screening platforms as those developed in this study have the potential to be useful tools for the large-scale functional characterisation of *P. falciparum* antigens, thereby facilitating the selection of new vaccine candidates.

5.5 BIBLIOGRAPHY

- Arévalo-Pinzón, G., Curtidor, H., Vanegas, M., Vizcaíno, C., Patarroyo, M. A., & Patarroyo, M. E. (2010). Conserved high activity binding peptides from the *Plasmodium falciparum* Pf34 rhoptry protein inhibit merozoites in vitro invasion of red blood cells. *Peptides*, *31*(11), 1987-94.
- Baksh, M. M., Kussrow, A. K., Mileni, M., Finn, M. G., & Bornhop, D. J. (2011). Label-free quantification of membrane-ligand interactions using backscattering interferometry. *Nature Biotechnology*, *29*(4), 357-60.
- Beckmann, R., Smythe, J. S., Anstee, D. J., & Tanner, M. J. (1998). Functional cell surface expression of band 3, the human red blood cell anion exchange protein (AE1), in K562 erythroleukemia cells: band 3 enhances the cell surface reactivity of Rh antigens. *Blood*, *92*(11), 4428-38.
- Bei, A. K., & Duraisingh, M. T. (2012). Functional analysis of erythrocyte determinants of *Plasmodium* infection. *International Journal for Parasitology*, *42*(6), 575-582.
- Bozdech, Z., Llinás, M., Pulliam, B. L., Wong, E. D., Zhu, J., & DeRisi, J. L. (2003). The transcriptome of the intraerythrocytic developmental cycle of *Plasmodium falciparum*. *PLoS Biology*, *1*(1), E5.
- de Brevern, A. G., Wong, H., Tournamille, C., Colin, Y., Le Van Kim, C., & Etchebest, C. (2005). A structural model of a seven-transmembrane helix receptor: the Duffy antigen/receptor for chemokine (DARC). *Biochimica et Biophysica Acta*, *1724*(3), 288-306.
- Camus, D., & Hadley, T. J. (1985). A *Plasmodium falciparum* antigen that binds to host erythrocytes and merozoites. *Science*, *230*(4725), 553-556.
- Chitinis, C. E. & Miller, H. M. (1994) Identification of the Erythrocyte Binding Domains of *Plasmodium vivax* and *Plasmodium knowlesi* Proteins Involved in Erythrocyte Invasion. *Journal of Experimental Medicine*, *180*(2), 497-506.
- Chitinis, C. E., Chaudhuri, A., Horuk, R., Pogo, A. O. & Miller H. M. (1996) The domain on the Duffy blood group antigen for binding *Plasmodium vivax* and *P. knowlesi* malarial parasites to erythrocytes. *Journal of Experimental Medicine*, *184*(4), 1531-6.
- Carter, R., Coulson, a, Bhatti, S., Taylor, B. J., & Elliott, J. F. (1995). Predicted disulfide-bonded structures for three uniquely related proteins of *Plasmodium falciparum*, Pfs230, Pfs48/45 and Pf12. *Molecular and Biochemical Parasitology*, *71*(2), 203-10.
- Clough, B., Paulitschke, M., Nash, G. B., Bayley, P. M., Anstee, D. J., Wilson, R. J. M., Pasvol, G., *et al.* (1995). Mechanism of regulation of malarial invasion by extraerythrocytic ligands. *Molecular and Biochemical Parasitology*, *69*(1), 19-27.

- Crompton, P., & Pierce, S. (2010). Advances and challenges in malaria vaccine development. *The Journal of Clinical Investigation*, 120(12), 4168-4178.
- Crosnier, C., Bustamante, L. Y., Bartholdson, S. J., Bei, A. K., Theron, M., Uchikawa, M., Mboup, S., *et al.* (2011). Basigin is a receptor essential for erythrocyte invasion by *Plasmodium falciparum*. *Nature*, 480(7378), 534-7.
- Desai, S. J., McCleskey, E. W., Schlesinger, P. H. and Krogstad, D. J. (1996). A novel pathway for Ca^{++} entry into *Plasmodium falciparum*-infected blood cells. *American Journal of Tropical Medicine and Hygiene*, 54(5), 464-470.
- Florens, L., Washburn, M. P., Raine, J. D., Anthony, R. M., Grainger, M., Haynes, J. D., Moch, J. K., *et al.* (2002). A proteomic view of the *Plasmodium falciparum* life cycle. *Nature*, 419(6906), 520-6.
- Geels, M. J., Imoukhuede, E. B., Imbault, N., van Schooten, H., McWade, T., Troye-Blomberg, M., Dobbelaer, R., *et al.* (2011). European Vaccine Initiative: lessons from developing malaria vaccines. *Expert Review of Vaccines*, 10(12), 1697-708.
- Gertow, K., Bellanda, M., Eriksson, P., Boquist, S., Hamsten, A., Sunnerhagen, M. & Fisher, R. M. (2004). Genetic and Structural Evaluation of Fatty Acid Transport Protein-4 in Relation to Markers of the Insulin Resistance Syndrome. *Journal of Clinical Endocrinology & Metabolism*, 89(1), 392-399.
- Goel, V. K., Li, X., Chen, H., Liu, S.-chun, Chishti, A. H., & Oh, S. S. (2003). Band 3 is a host receptor binding merozoite surface protein 1 during the *Plasmodium falciparum* invasion of erythrocytes. *Proceedings of the National Academy of Sciences of the United States of America*, 100(9), 5164-69.
- Graham, F. L., Smiley, J., Russell, W.C. & Nairn, N. (1977) Characteristics of a human cell line transformed by DNA from human adenovirus type 5. *The Journal of General Virology*, 36(1), 59-74.
- Greenwood, B. M., & Targett, G. A. T. (2011). Malaria vaccines and the new malaria agenda. *Clinical Microbiology and Infection*, 17(11), 1600-7.
- Hassoun, H., Hanada, T., Lutchman, M., Sahr, K. E., Palek, J., Hanspal, M., & Chishti, A. H. (1998). Complete deficiency of glycophorin A in red blood cells from mice with targeted inactivation of the band 3 (AE1) gene. *Blood*, 91(6), 2146-51.
- Hofmann, K. and Stoffel, W. (1993) TMbase- A database of membrane spanning protein segments. *Biological Chemistry Hoppe-Seyler*, 374, 166-169.
- Kadekoppala, M., Ogun, S. A., Howell, S., Gunaratne, R. S., & Holder, A. A. (2010). Systematic genetic analysis of the *Plasmodium falciparum* MSP7-like family reveals differences in

- protein expression, location, and importance in asexual growth of the blood-stage parasite. *Eukaryotic Cell*, 9(7), 1064-74.
- Kakhniashvili, D. G., Bulla, L. A., & Goodman, S. R. (2004). The human erythrocyte proteome: analysis by ion trap mass spectrometry. *Molecular & Cellular Proteomics*, 3(5), 501-9.
- King, C. L., Adams, J. H., Xianli, J., Grimberg, B. T., McHenry, A. M., Greenberg, L. J., Siddiqui, A., *et al.* (2011). Fy(a)/Fy(b) antigen polymorphism in human erythrocyte Duffy antigen affects susceptibility to *Plasmodium vivax* malaria. *Proceedings of the National Academy of Sciences of the United States of America*, 108(50), 20113-8.
- Klar, J., Schweiger, M., Zimmerman, R., Zechner, R., Li, H., Törmä, H., Vahlquist, A., *et al.* (2009). Mutations in the fatty acid transport protein 4 gene cause the ichthyosis prematurity syndrome. *American Journal of Human Genetics*, 85(2), 248-53.
- Koppel, D. E., Sheetz, M. P., & Schindlert, M. (1981). Matrix control of protein diffusion in biological membranes. *Biophysics*, 78(6), 3576-3580.
- Krogh, A., Larsson, B., von Heijne, G. and Sonnhammer, E.L.L. (2001) Predicting transmembrane protein topology with a hidden Markov model: Application to complete genomes. *Journal of Molecular Biology*., 305, 567-580
- Larkin, M. A., Blackshields, G., Brown, N. P., Chenna, R., McGettigan, P. A., McWilliam, H., *et al.* (2007) Clustal W and Clustal X version 2.0. *Bioinformatics*, 23(21), 2947-8
- Maier, A. G., Duraisingh, M. T., Reeder, J. C., Patel, S. S., Kazura, J. W., Zimmerman, P. A., & Cowman, A. F. (2002). *Plasmodium falciparum* erythrocyte invasion through glycophorin C and selection for Gerbich negativity in human populations. *Nature Medicine*, 9(1), 87-92.
- Mayer, D. C., Kaneko, O., Hudson-Taylor, D. E., Reid, M. E., & Miller, L. H. (2001). Characterization of a *Plasmodium falciparum* erythrocyte-binding protein paralogous to EBA-175. *Proceedings of the National Academy of Sciences of the United States of America*, 98(9), 5222-7.
- Maynard, J., Lindquist, N., Sutherland, N., Lesuffleur, A., Warrington, A., Rodriguez, M., & Oh, S.-H. (2009). Next generation SPR technology of membrane-bound proteins for ligand screening and biomarker discovery. *Biotechnology Journal*, 4(11), 1542-1558.
- Miller, L H, Hudson, D., Renner, J., Taylor, D., Hadley, T. J., & Zilberstein, D. (1983). A monoclonal antibody to rhesus erythrocyte band 3 inhibits invasion by malaria (*Plasmodium knowlesi*) merozoites. *The Journal of Clinical Investigation*, 72(4), 1357-64.
- Murphy, S. C., Hiller, N. L., Harrison, T., Lomasney, J. W., Mohandas, N., & Haldar, K. (2006). Lipid rafts and malaria parasite infection of erythrocytes. *Molecular Membrane Biology*, 23(1), 81-8.

- Ménard, D., Barnadas, C., Bouchier, C., Henry-Halldin, C., Gray, L. R., Ratsimbaoa, A., Thonier, V., et al. (2010). *Plasmodium vivax* clinical malaria is commonly observed in Duffy-negative Malagasy people. *Proceedings of the National Academy of Sciences of the United States of America*, 107(13), 5967-71.
- Narum, D. L., Fuhrmann, S. R., Luu, T., & Sim, B. K. L. (2002). A novel *Plasmodium falciparum* erythrocyte binding protein-2 (EBP2/BAEBL) involved in erythrocyte receptor binding. *Molecular and Biochemical Parasitology*, 119(2), 159-68.
- Obando-Martinez, A. Z., Curtidor, H., Arévalo-Pinzón, G., Vanegas, M., Vizcaino, C., Patarroyo, M. A., & Patarroyo, M. E. (2010). Conserved high activity binding peptides are involved in adhesion of two detergent-resistant membrane-associated merozoite proteins to red blood cells during invasion. *Journal of Medicinal Chemistry*, 53(10), 3907-18.
- Ota, K., Sakaguchi, M., Hamasaki, N., & Mihara, K. (1998). Assessment of topogenic functions of anticipated transmembrane segments of human band 3. *The Journal of Biological Chemistry*, 273(43), 28286-91.
- Barnwell, J.W., Nichols, M. E. & Rubinstein, P. (1989). *In vitro* evaluation of the role of the Duffy blood group in erythrocyte invasion by *Plasmodium vivax*. *Journal of Experimental Medicine*, 169 (5), 1795-802.
- Pasini, E. M., Mann, M., & Thomas, A. W. (2010). Red blood cell proteomics, Protéomique du globule rouge. *Transfusion Clinique et Biologique*, 17(3), 151-164.
- Pasini, E. M., Kirkegaard, M., Mortensen, P., Lutz, H. U., Thomas, A. W., & Mann, M. (2006). In-depth analysis of the membrane and cytosolic proteome of red blood cells. *Blood*, 108(3), 791-801.
- Pearce, J. A., Mills, K., Triglia, T., Cowman, A. F., & Anders, R. F. (2005). Characterisation of two novel proteins from the asexual stage of *Plasmodium falciparum*, H101 and H103. *Molecular and Biochemical Parasitology*, 139(2), 141-51.
- Polley, M. J., Phillips, M. L., Wayner, E., Nudelman, E., Singhal, A. K., Hakomori, S., Paulson, J.C. (1991) CD62 and endothelial cell-leukocyte adhesion molecule 1 (ELAM-1) recognize the same carbohydrate ligand, sialyl-Lewis x. *Proceedings of the National Academy of Sciences of the United States of America*, 88(14), 6224-8.
- Proellocks, N. I., Kovacevic, S., Ferguson, D. J. P., Kats, L. M., Morahan, B. J., Black, C. G., Waller, K. L., et al. (2007). *Plasmodium falciparum* Pf34, a novel GPI-anchored rhoptry protein found in detergent-resistant microdomains. *International Journal for Parasitology*, 37(11), 1233-41.
- Sanders, P. R., Gilson, P. R., Cantin, G. T., Greenbaum, D. C., Nebl, T., Carucci, D. J., McConville, M. J., et al. (2005). Distinct protein classes including novel merozoite surface

antigens in Raft-like membranes of *Plasmodium falciparum*. *The Journal of Biological Chemistry*, 280(48), 40169-76.

Sikora, C. W., & Turner, R. J. (2005). Investigation of ligand binding to the multidrug resistance protein EmrE by isothermal titration calorimetry. *Biophysical Journal*, 88(1), 475-82.

Silmon de Monerri, N. C., Flynn, H. R., Campos, M. G., Hackett, F., Koussis, K., Withers-Martinez, C., Skehel, J. M., et al. (2011). Global identification of multiple substrates for *Plasmodium falciparum* SUB1, an essential malarial processing protease. *Infection and Immunity*, 79(3), 1086-97.

Singh, S., Soe, S., Weisman, S., Barnwell, J. W., Pérignon, J. L., & Druilhe, P. (2009). A conserved multi-gene family induces cross-reactive antibodies effective in defense against *Plasmodium falciparum*. *PloS One*, 4(4), e5410.

Speicher, D. W. (2006). Deep mining of the RBC proteome. *Blood*, 108(3), 779-780.

Tham, W.-H., Healer, J., & Cowman, A. F. (2012). Erythrocyte and reticulocyte binding-like proteins of *Plasmodium falciparum*. *Trends in Parasitology*, 28(1), 23-30.

Tham, W.-H., Wilson, D. W., Reiling, L., Chen, L., Beeson, J. G., & Cowman, A. F. (2009). Antibodies to reticulocyte binding protein-like homologue 4 inhibit invasion of *Plasmodium falciparum* into human erythrocytes. *Infection and Immunity*, 77(6), 2427-35.

Timmann, C., Thyé, T., Vens, M., Evans, J., May, J., Ehmen, C., Sievertsen, J., et al. (2012). Genome-wide association study indicates two novel resistance loci for severe malaria. *Nature*, 489(7416), 443-6

Tomishige, M., Sako, Y., & Kusumi, A. (1998). Regulation Mechanism of the Lateral Diffusion of Band 3 in Erythrocyte Membranes by the Membrane Skeleton. *Cell*, 142(4), 989-1000.

Tran, T. M., Moreno, A., Yazdani, S. S., Chitnis, C. E., Barnwell, J. W., & Galinski, M. R. (2005). Detection of a *Plasmodium vivax* erythrocyte binding protein by flow cytometry. *Cytometry. Part A: the Journal of the International Society for Analytical Cytology*, 63(1), 59-66.

Tsunady, G.E. and Simon, I. (2001) The HMMTOP transmembrane topology prediction server. *Bioinformatics*, 8, 849-850

Wang, D. N., Kühlbrandt, W., Sarabia, V. E., & Reithmeier, R. A. (1993). Two-dimensional structure of the membrane domain of human band 3, the anion transport protein of the erythrocyte membrane. *The EMBO Journal*, 12(6), 2233-9.

Wickramarachchi, T., Devi, Y. S., Mohammed, A., & Chauhan, V. S. (2008). Identification and characterization of a novel *Plasmodium falciparum* merozoite apical protein involved in erythrocyte binding and invasion. *PloS One*, 3(3), e1732.

Wright, G. J. (2009). Signal initiation in biological systems: the properties and detection of transient extracellular protein interactions. *Molecular BioSystems*, 5, 1405-1412.